CHAPTER 3

RESULTS AND DISCUSSION

3.1 POWDERS CHARACTERIZATION

PZT and PLZT powders synthesized from both nitrate solutions and hydrothermal process were characterized by the following methods.

3.1.1 INVESTIGATION OF THERMAL DECOMPOSITION

3.1.1.1 PZT Powders from Nitrate Solutions

The thermal decomposition of the intermediate products from nitrate solutions is illustrated in Figure 3.1. The curves of thermogravimetric (TGA) and differential thermal analysis (DTA) exhibited the first weight loss of 12.06 percent accompanied by endothermic peak around 110 °C. This weight loss was related to the elimination of both associated water and low boiling point organic residues from the starting zirconium and titanium precursor solutions such as $[O(CH_2)_2CH_3]_4$ in zirconium n-propoxide and $[OCH(CH_2)_2]_4$ in titanium isopropoxide. The second endothermic peak occurred around 400 °C at the weight loss of 6.82 percent was associated with the evolution of gasses such as NH_3, NO or NO_2[5, 6]. The small exothermic peak around 550 °C of 1.23 percent weight loss could be attributed to the heat of crystallization of PZT[86]. The total weight loss from the elimination of water and the combustion of organic and inorganic residues was 20.11 percent and the thermal decomposition was almost completed at temperature above 600°C.

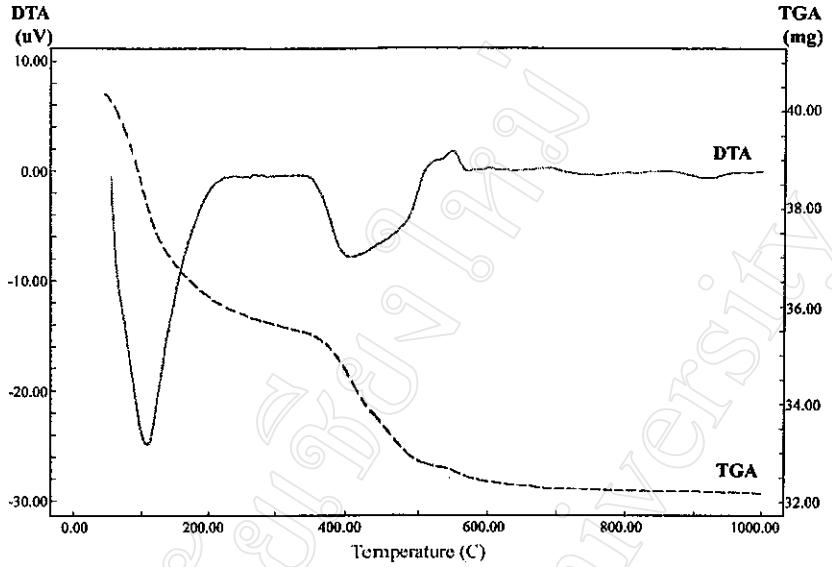

Figure 3.1 Thermogravimetric and differential thermal analysis of PZT powders synthesized by nitrate solutions

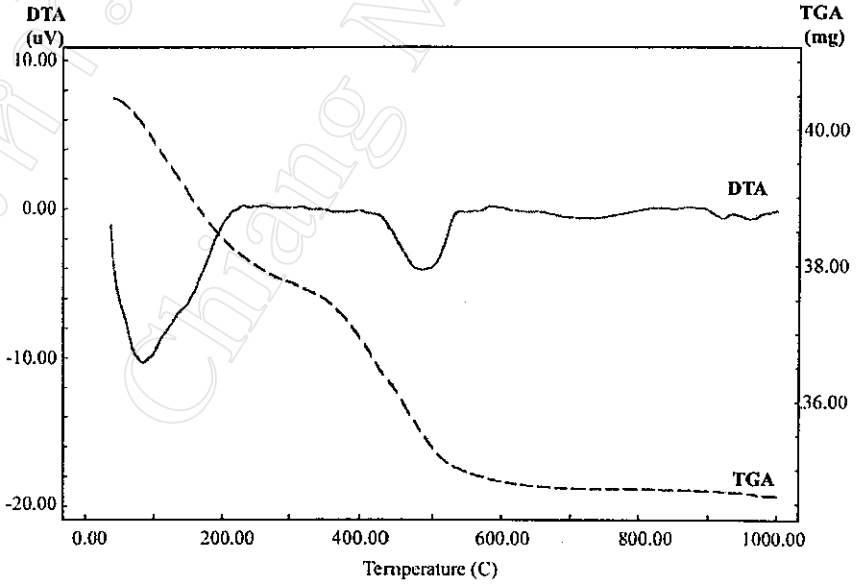

Figure 3.2 Thermogravimetric and differential thermal analysis of PLZT powders synthesized by nitrate solutions

Figure 3.2 shows the thermogravimetric analysis and differential thermal analysis of PLZT powders synthesized by nitrate solutions. The TGA and DTA curves exhibited the same results as Figure 3.1. The overall weight loss was 14.36 percent and the weight loss was almost completed at temperature above 600 °C. Further weight loss at temperature over 900 °C might be due to the evaporation of lead oxide[87].

3.1.1.2 PZT Powders from Hydrothermal Process

The TGA-DTA curves of the intermediate PZT hydrothermal product are shown in Figure 3.3. This picture showed two endothermic peaks associated with two TGA weight loss regions at about 80 °C and 930 °C. Between 300 and 900 °C the weight loss was stable. The first weight loss was attributed to the desorption of surface adsorbed hydroxyl group, which possessed various bonding energies with the surface owing to their adsorption on several surface sites with different coordination numbers and mostly desorbing at about 100 °C[88]. The second small endothermic peak at around 350 °C was due to the dissociation of organic group, mainly acetate and propoxide groups bonded to the zirconium and titanium atoms. The last endothermic peak occurred around 900 to 1000 °C was due to the evaporation of PbO in PZT powders[87]. The overall weight loss was 3.20 percent.

Figure 3.4 shows thermogravimetric analysis and differential thermal analysis of PLZT powders synthesized by hydrothermal process. The TGA and DTA curves exhibited the same results as Figure 3.3. The overall weight loss was 4.67 percent.

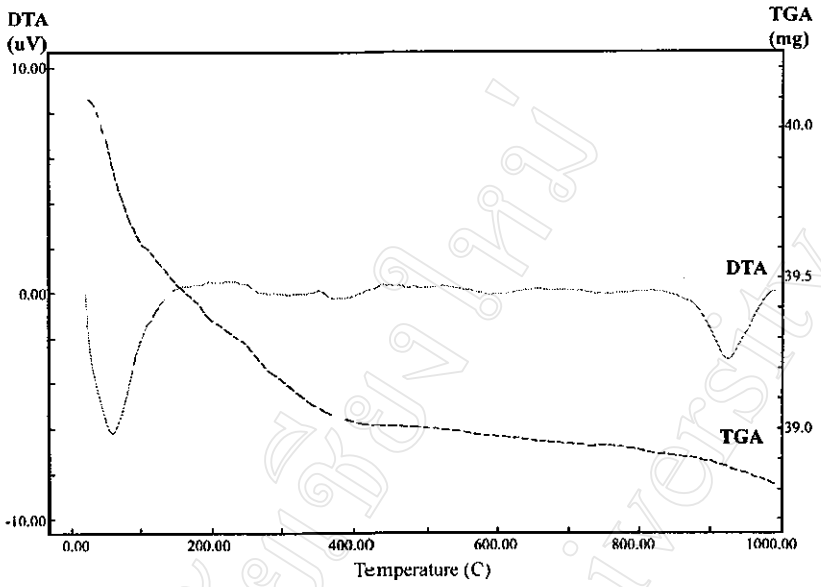

Figure 3.3 Thermogravimetric and differential thermal analysis of PZT powders synthesized by hydrothermal process.

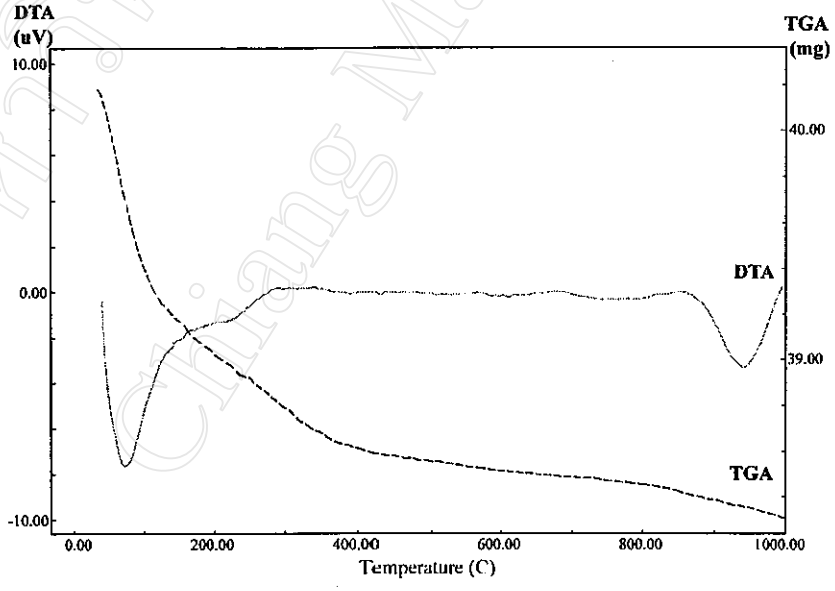

Figure 3.4 Thermogravimetric and differential thermal analysis of PLZT powders synthesized by hydrothermal process.

3.1.2 CRYSTALLINE STRUCTURE DETERMINATION

3.1.2.1 PZT Powders from Nitrate Solutions

The XRD patterns of PZT powders obtained through the freeze drying route are shown in Figure 3.5. The powders were calcined at temperature between 550 °C and 800 °C for 2 hours at intervals of 50 °C.

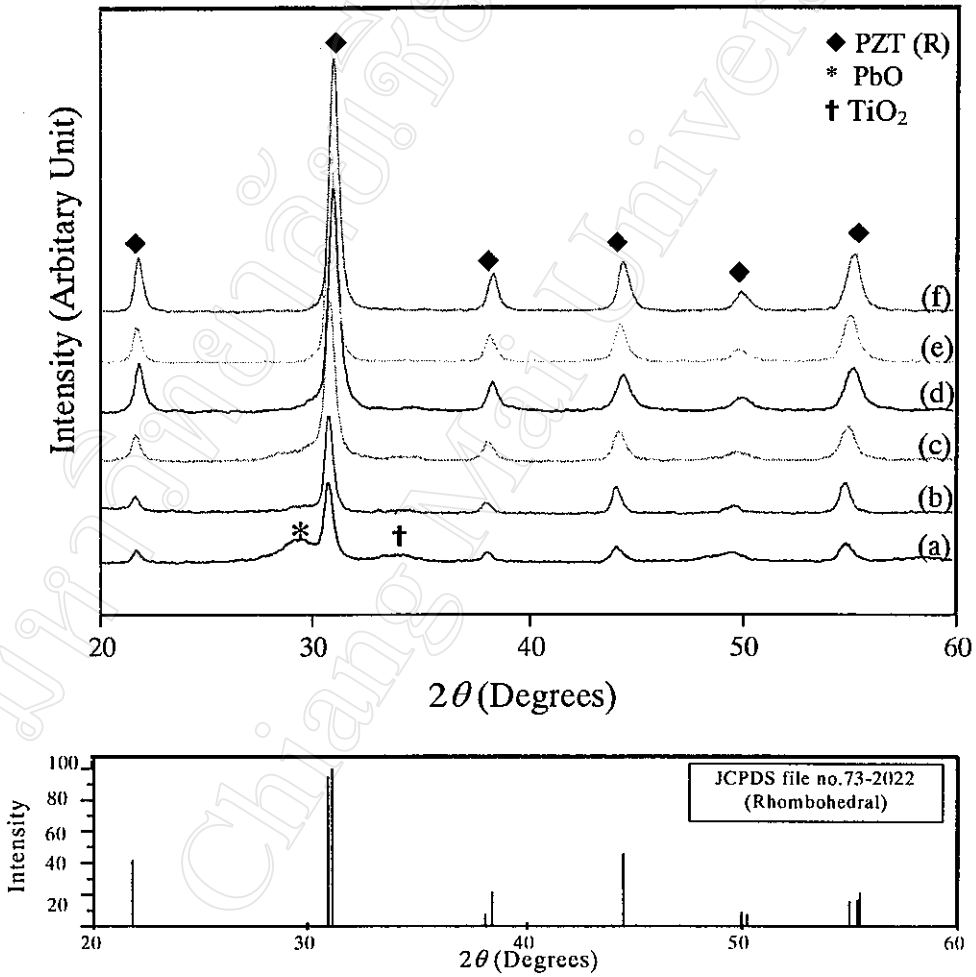

Figure 3.5 XRD patterns of PZT powders obtained from freeze drying process calcined at (a) 550 °C, (b) 600 °C, (c) 650 °C, (d) 700 °C, (e) 750 °C and (f) 800 °C for 2 hours.

Calcined powders at 550 °C for 2 hours showed perovskite PZT which was composed of PbO (2θ~29 degrees) and TiO_2 at 2θ~34 degrees. At higher calcination temperature, PbO and TiO_2 peaks tended to be decreased. Above 600 °C, no appearance of PbO peak and phase pure of rhombohedral PZT was formed (JCPDS file number 73-2022).

For PZT powders obtained from coprecipitation (Figure 3.6), the PbO peak were still appeared until the calcination temperature of 600 °C.

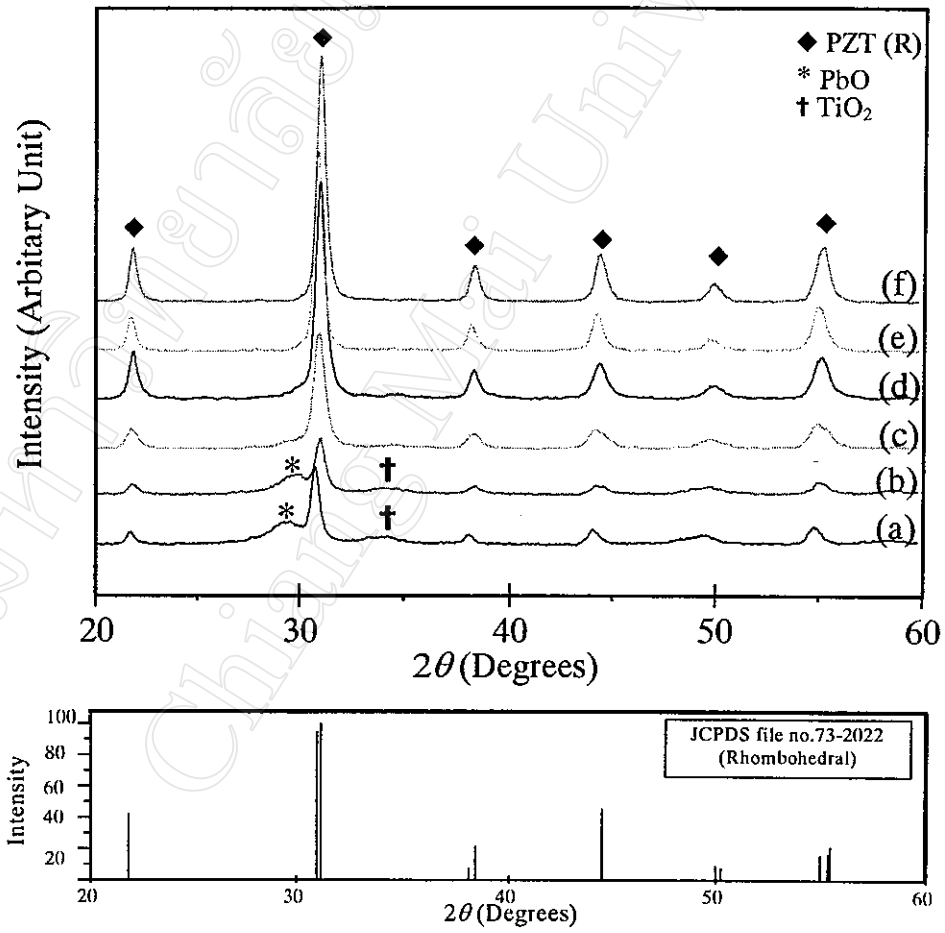

Figure 3.6 XRD patterns of PZT powders obtained from coprecipitation process calcined at (a) 550 °C, (b) 600 °C, (c) 650 °C, (d) 700 °C, (e) 750 °C and (f) 800 °C for 2 hours.

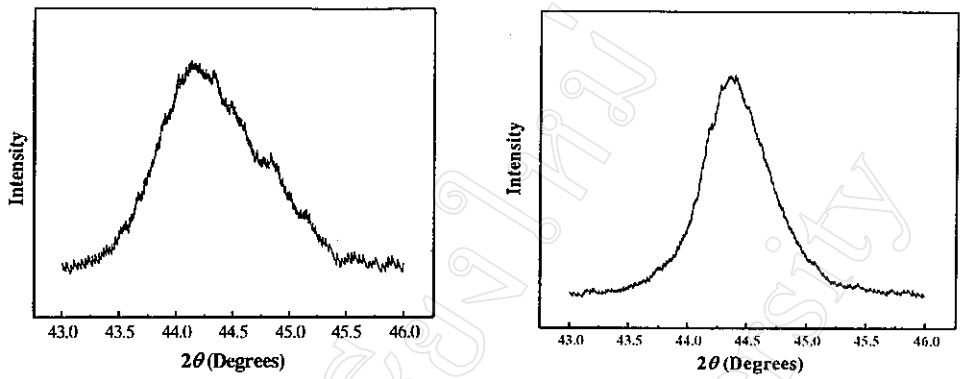

Figure 3.7 XRD patterns of PZT powders obtained from coprecipitation process at various calcination temperatures of (a) 650 °C and (b) 800 °C for 2 hours

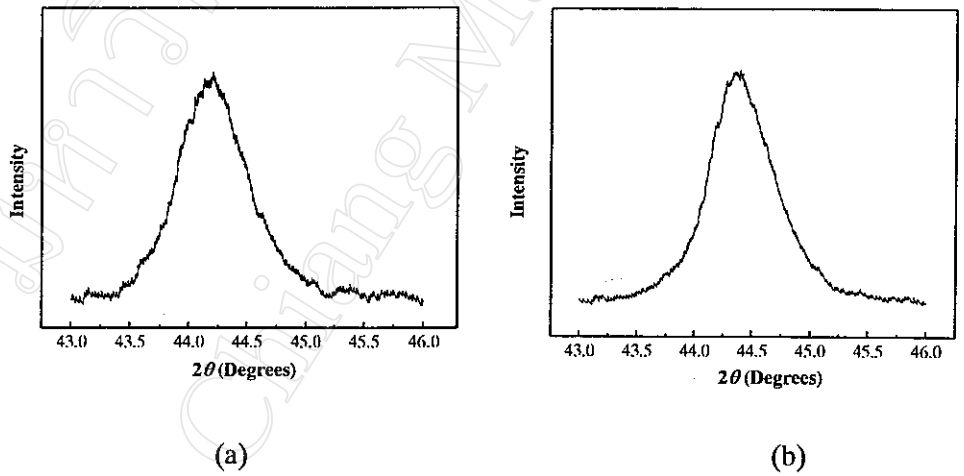

Figure 3.8 XRD patterns of PZT powders obtained from freeze drying process at various calcination temperatures of (a) 600 °C and (b) 800 °C for 2 hours

For coprecipitation process, calcined powders at 650, 700, 750 and 800 °C for 2 hours showed perovskite phase pure of PZT powders. At calcination temperature of 550 °C and 600 °C, PbO and TiO_2 occurred together with perovskite PZT phase. Phase pure of rhombohedral PZT was formed at calcination temperature of 650 °C and higher. These XRD patterns showed that freeze-drying process was slightly affective than coprecipitation process.

The structure of PZT powders could be investigated by the peak at $2\theta \sim 45$ degrees[89]. Figure 3.7(a) shows PZT powders obtained from coprecipitation process calcined at 650 °C for 2 hours, broad peak indicated some impurities within the structure. At higher calcination temperature (800 °C for 2 hours), pure rhombohedral phase was formed (Figure 3.7(b)).

For freeze drying process, only phase pure of rhombohedral was formed at the calcining temperature of 600 °C for 2 hours (Figure 3.8 (a)). And still be in rhombohedral phase as high calcining temperature as 800 °C, as shown in Figure 3.8(b).

3.1.2.2 PLZT Powders from Nitrate Solutions

The XRD patterns of PLZT powders which contained 10 mole% La, calcined at temperature between 550 °C to 800 °C for 2 hours obtained through the coprecipitation process is illustrated in Figure 3.9. PbO and TiO_2 peaks occurred at calcination temperature of 550 °C and 600 °C, above 650 °C, perovskite phase was formed as a major phase in PLZT powders. The results confirmed that the PLZT was

in the cubic form after calcined at 650 to 800 °C which matched with the JCPDS file number 46-0336.

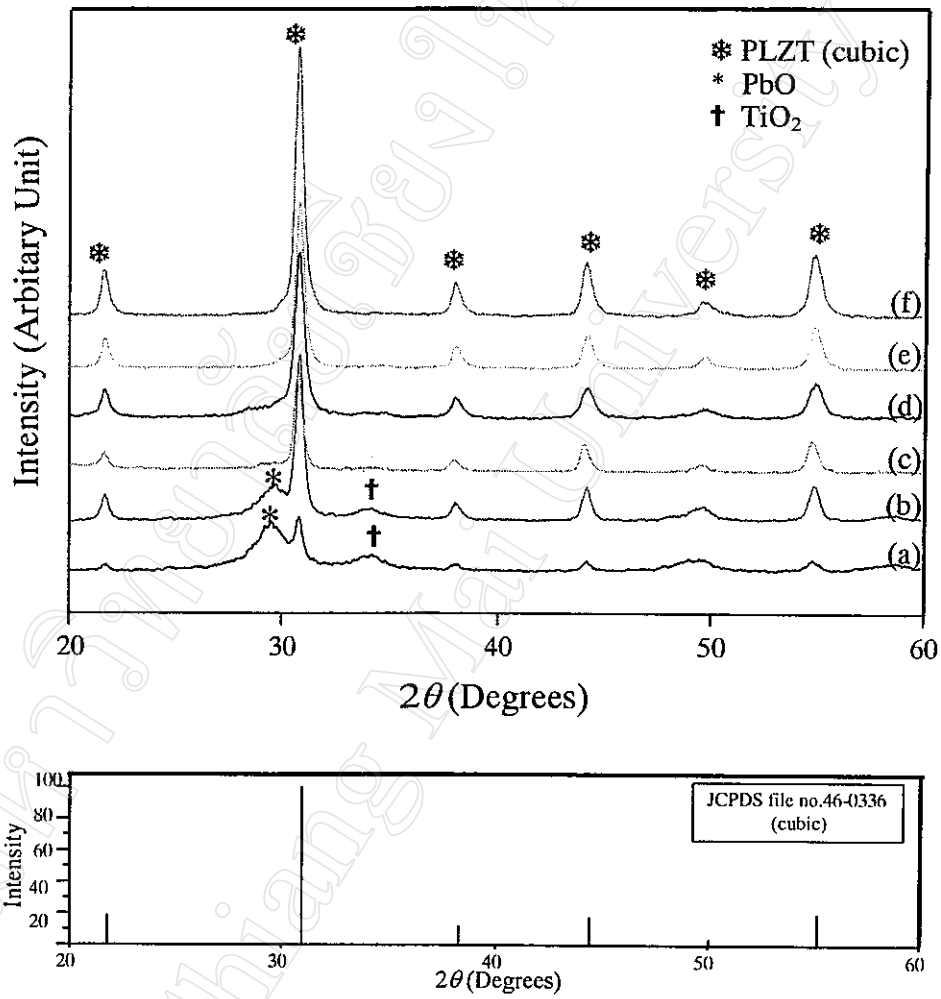

Figure 3.9 XRD patterns of PLZT powders obtained from coprecipitation process calcined at (a) 550 °C, (b) 600 °C, (c) 650 °C, (d)700 °C, (e) 750 °C and (f) 800 °C for 2 hours.

3.1.2.3 PZT Powders from Hydrothermal Process

3.1.2.3.1 Effect of Mineralizer Concentration

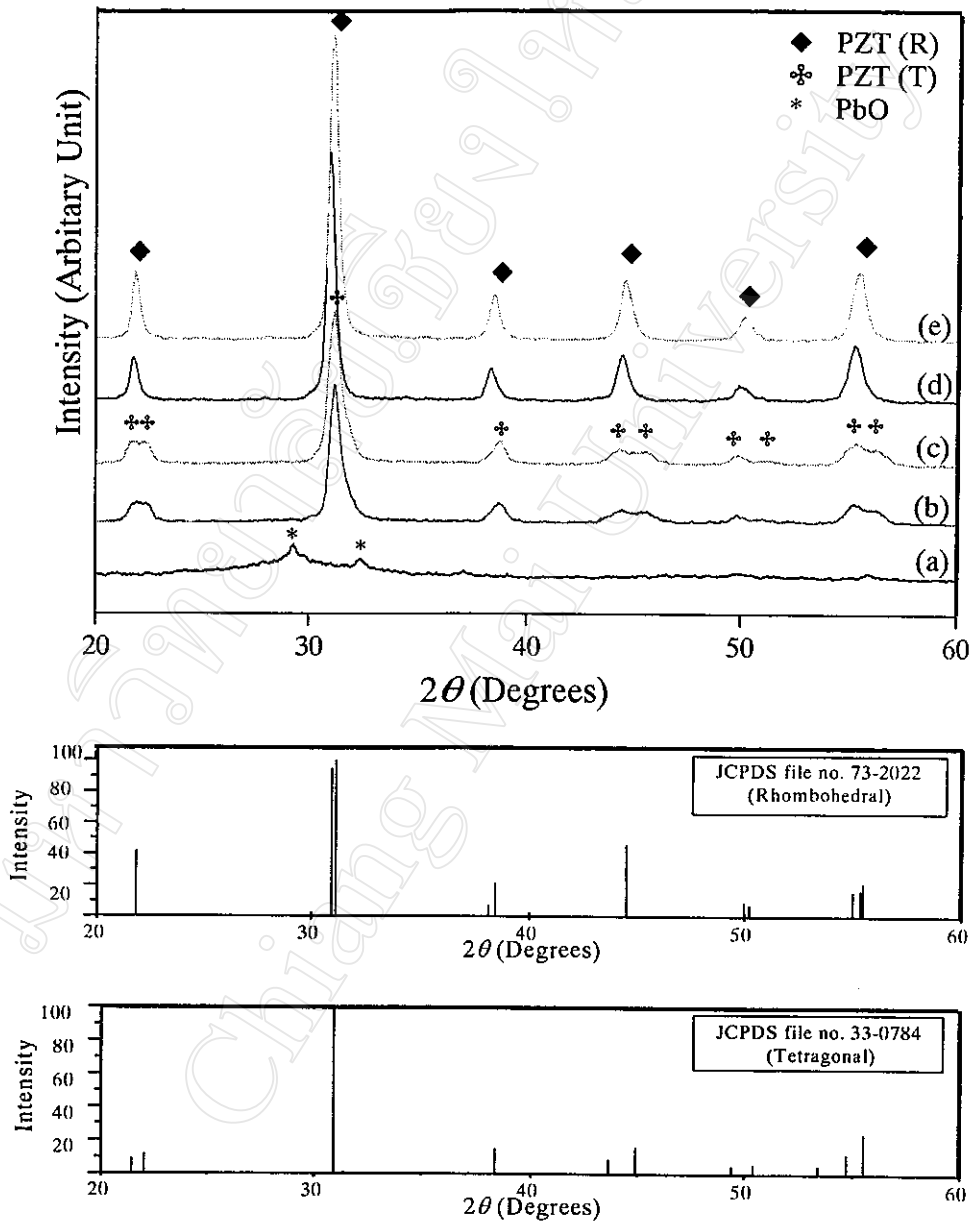

Figure 3.10 XRD patterns of PZT powders synthesized by hydrothermal process at different KOH concentrations as (a) 1.0 M KOH, (b) 2.0 M KOH, (c) 3.0 M KOH, (d) 4.0 M KOH and (e) 5.0 M KOH

The effect of mineralizer concentration on hydrothermally synthesized PZT powders is given in Figure 3.10. The synthesis time was fixed at 6 hours while the synthesis temperature was 200 °C. At low KOH concentration (1.0 M KOH), the product was amorphous and some PbO peaks occurred. At higher KOH concentration phase pure perovskite PZT was formed. At 2.0 M and 3.0 M KOH, perovskite PZT had a tetragonal structure as shown from the peak splitting around $2\theta \sim 45$ degrees in XRD patterns (JCPDS file number 33-0784). At relatively high concentration (4.0 M and 5.0 M KOH), tetragonal perovskite PZT were transformed to the rhombohedral form. The results indicated that the PZT composition shifted to the $PbZrO_3$ rich side of the PZT phase diagram (Figure 1.6) as the concentration of KOH increased.

3.1.2.3.2 Effect of Mineralizer Type

The effect of mineralizer type on hydrothermally synthesized PZT powders is shown in Figure 3.11. The synthesis time was fixed at 6 hours, the synthesis temperature was 200 °C, and NaOH at concentration of 1.0 to 4.0 M was used as a mineralizer. The XRD showed the same patterns as Figure 3.10. The product was amorphous, with the appearance of some PbO peaks, at 1.0 M NaOH. At 2.0 M and 3.0 M NaOH, tetragonal PZT was formed and at 4.0 M NaOH, tetragonal PZT transformed to rhombohedral PZT. XRD pattern of PZT powders synthesized from 4.0 M KOH is also shown in Figure 3.11, and from Figure 3.10 and 3.11, there were no different between these two figures. So we can use either NaOH or KOH as the mineralizer in a similar concentration for hydrothermally synthesized perovskite PZT powders. And these results indicated that mineralizer concentration was one of the important factors for hydrothermal synthesis.

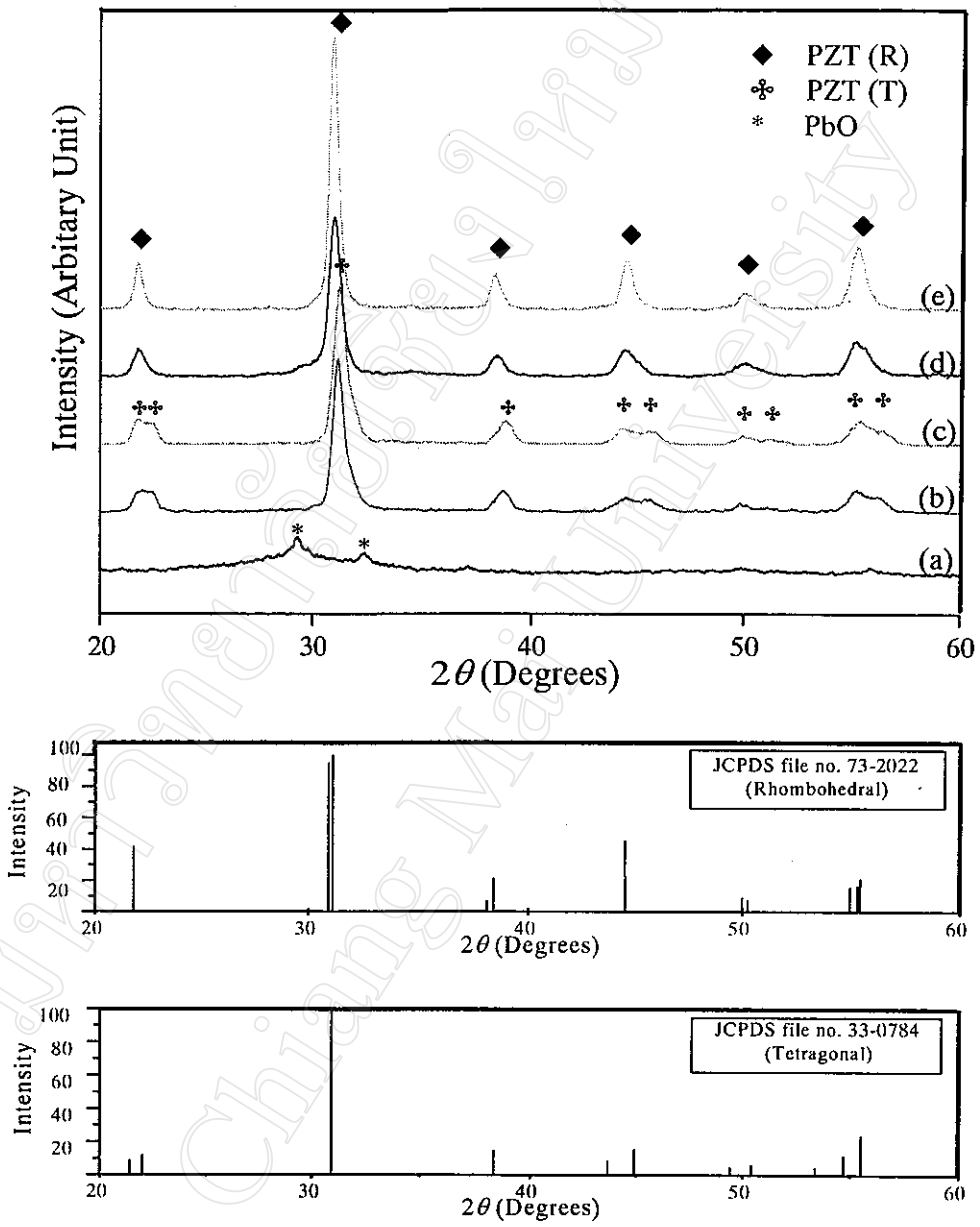

Figure 3.11 XRD patterns of PZT powders synthesized by hydrothermal process at different NaOH concentrations as (a) 1.0 M NaOH, (b) 2.0 M NaOH, (c) 3.0 M NaOH, (d) 4.0 M NaOH and (e) PZT powders synthesized by hydrothermal process using 4.0 M KOH

3.1.2.3.3 Effect of pH Value

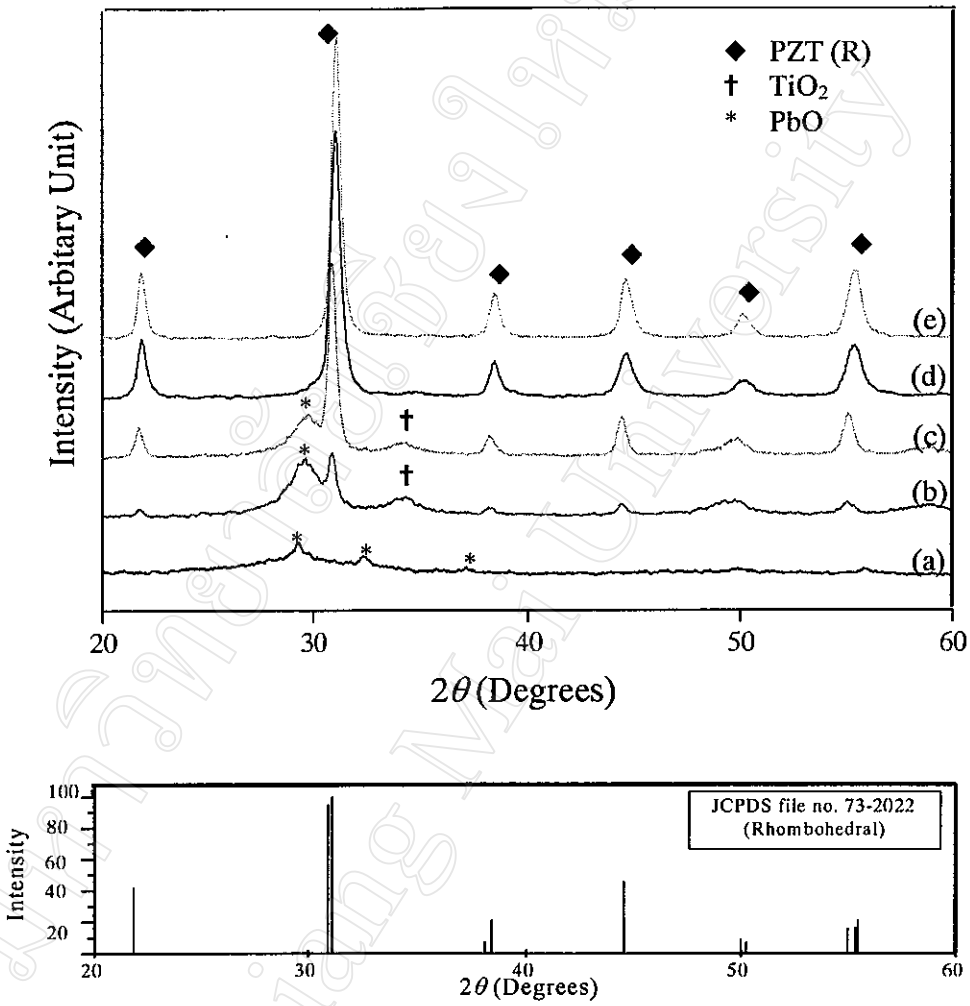

Figure 3.12 XRD patterns of PZT powders synthesized by hydrothermal process using KOH as a mineralizer at different pH values as (a) pH 10, (b) pH 11, (c) pH 12, (d) pH 13 and (e) pH 14

The effect of pH values on hydrothermally synthesized PZT powders is illustrated in Figure 3.12. The synthesis time was fixed at 6 hours while the synthesis temperature was 200 °C. 4.0 M KOH at various pH values was used as mineralizer (pH value varied from 10 to 14). At low pH value (at pH 10), the product was amorphous. And at relalive high pH values (pH 11 and 12), the products were composed of PbO and TiO_2. Perovskite phase PZT was formed at higher pH values. The critical pH value required for perovskite PZT formation was 13. At pH 13 and 14, perovskite phase PZT was formed completely. Rhombohedral phase was occurred as a major phase in the XRD patterns.

3.1.2.3.4 Effect of Synthesis Time

The effect of synthesis time on perovskite PZT formation is shown in Figure 3.13. The synthesis temperature was fixed at 200 °C and 4.0 M KOH was used as a mineralizer. The synthesis time was varied from 2 to 48 hours. At 2 and 4 hours, the XRD patterns showed no obvious of perovskite PZT, the products were amorphous and composed of TiO_2 and PbO. Above 6 hours, phase pure perovskite rhombohedral PZT was formed. It can be seen clearly from the XRD patterns that the critical synthesis time for PZT powders by hydrothermal process at this condition was 6 hours. Rhombohedral PZT was formed at the synthesis time of 6 hours and longer.

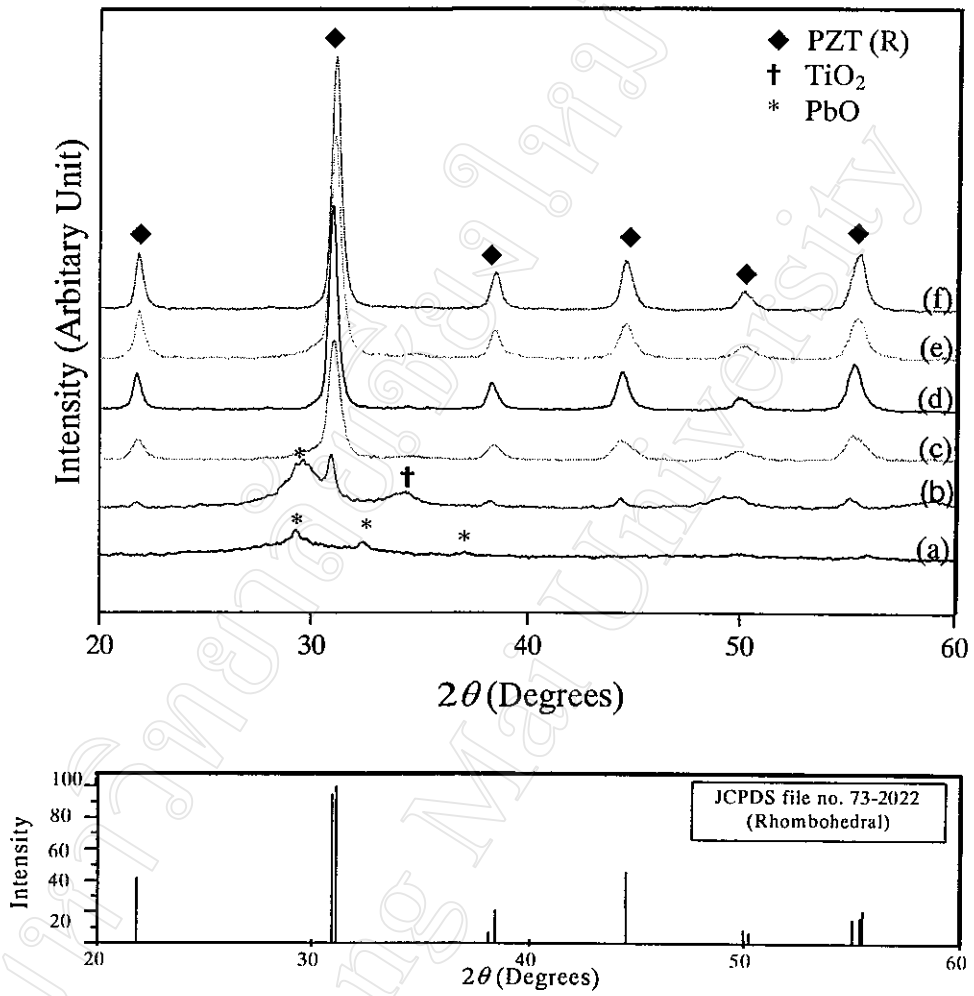

Figure 3.13 XRD patterns of PZT powders synthesized by hydrothermal process at 200 °C using 4.0 M KOH as a mineralizer at different synthesis times as (a) 2 h, (b) 4 h, (c) 6 h, (d) 12 h, (e) 24 h and (f) 48 h

3.1.2.3.5 Effect of Synthesis Temperature and Time

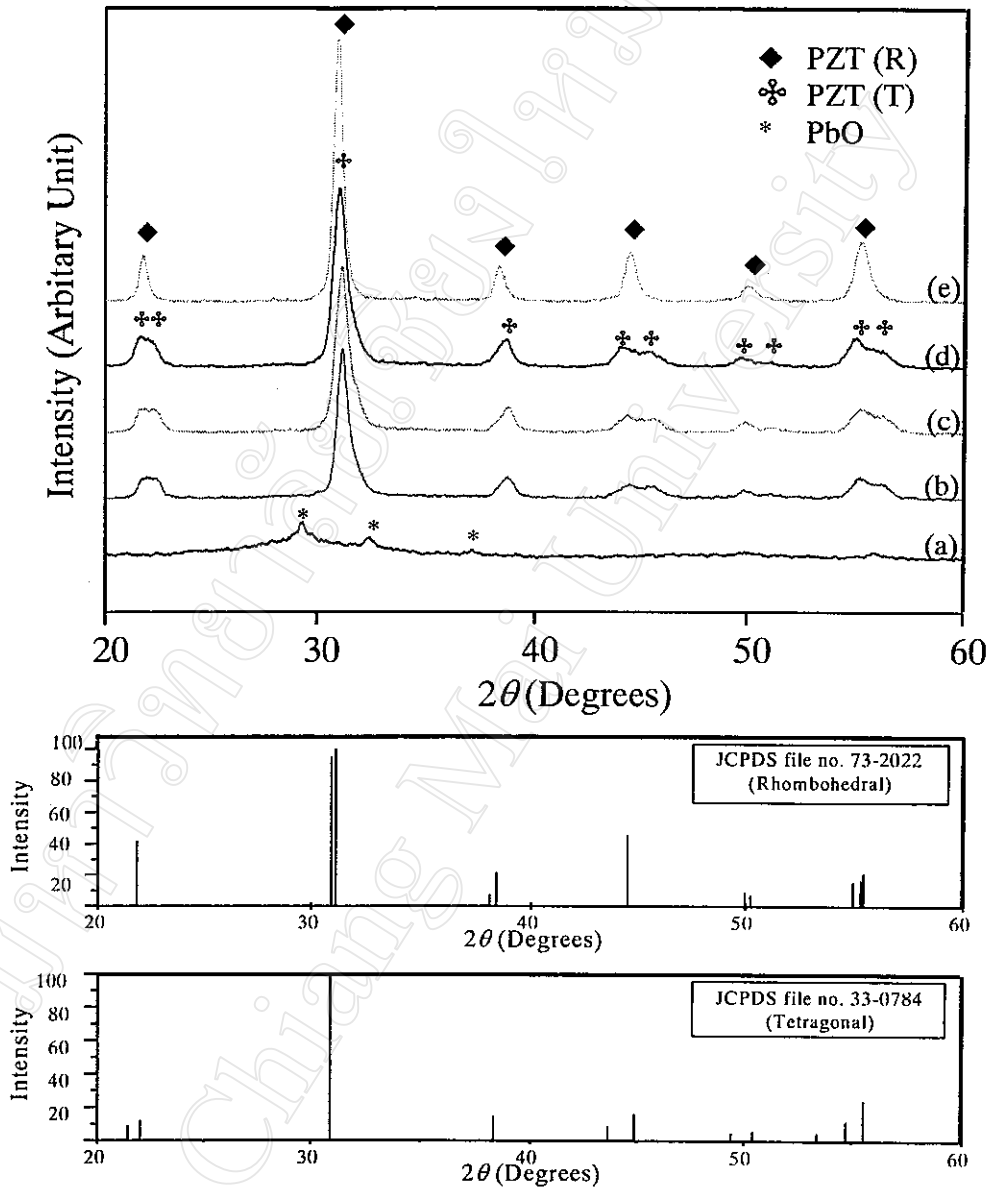

Figure 3.14 XRD patterns of PZT powders synthesized by hydrothermal process using 4.0 M KOH as a mineralizer at different synthesis temperatures and times as (a) 50 °C, 48 h, (b) 100 °C, 48 h, (c) 150 °C, 6 h, (d) 150 °C, 24 h and (e) 200 °C, 6 h

Figure 3.14 shows XRD patterns of PZT powders synthesized by hydrothermal process using 4.0 M KOH as a mineralizer at different synthesis temperatures and times. At relatively low synthesis temperature (at 50°C) the product was amorphous with some appearance of PbO peaks even the synthesis time as long as 48 hours, [Figure 3.14(a)]. At low synthesis temperature (at 100 °C) and synthesis time of 48 hours, the product was in the form of tetragonal PZT. At relatively high synthesis temperature (at 150 °C) and synthesis time of 6 hours, Figure 3.14 (c), the product was tetragonal PZT and still be in this form as longer synthesis time as 24 hours, [Figure 3.14 (d)]. At high synthesis temperature of 200 °C, the product shifted to the zirconium rich side in the MPB phase, the pattern indicated rhombohedral PZT product. From this study, it can be seen clearly that the synthesis temperature was one of the major effects in the perovskite hydrothermally synthesized PZT powders.

3.1.2.4 PLZT Powders from Hydrothermal Process

XRD pattern of PLZT powders at the different mole %La synthesized by hydrothermal process at 200 °C for 6 hours using 4.0 M KOH at pH 14 as a mineralizer is given in Figure 3.15. From XRD patterns, cubic phase of PLZT was occurred and matched with the JCPDS file number 46-0336. The desired PLZT compositions were 0.92:0.08:0.65:0.35, 0.91:0.09:0.65:0.35, 0.90:0.10:0.65:0.35 and 0.88:0.12: 0.65:0.35 for 8%, 9%, 10% and 12% PLZT respectively

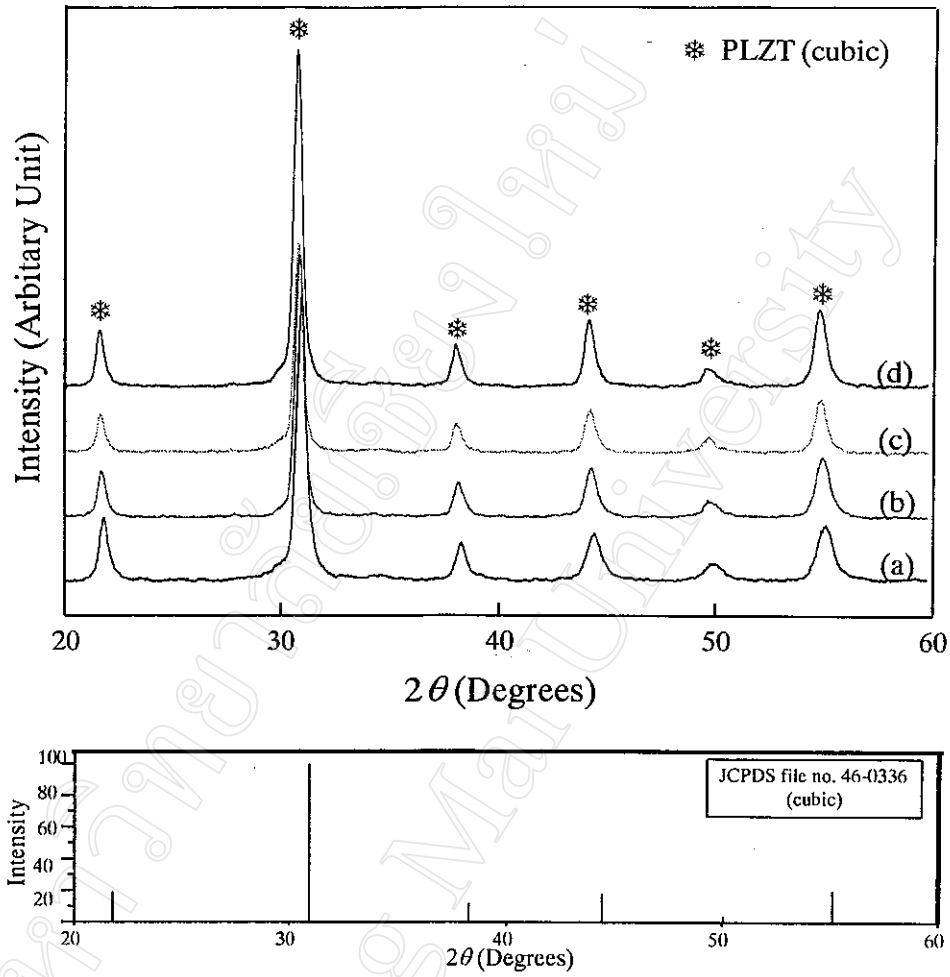

Figure 3.15 XRD patterns of PLZT powders synthesized by hydrothermal process at 200 °C for 6 hours using 4.0 M KOH as a mineralizer in different mole% La at (a) 8 %La, (b) 9 %La, (c) 10 %La and (d) 12 %La.

3.1.3 MICROSTRUCTURE ANALYSIS

3.1.3.1 PZT Powders from Nitrate Solutions

SEM micrograps of PZT powders obtained from freeze-drying process and coprecipitation process at different calcining temperatures are shown in Figure 3.16 [(a)-(f)]. For both processes, as calcining temperature increased, the particle size and the extent of particle agglomeration increased significantly. It can be seen from Figure 3.16 [(a)-(c)], at calcining temperature of 600 °C for 2 hours, the micrograph showed spherical particles that were 0.17 μm to 0.25 μm in diameter. At 700 °C, the particles became larger with sizes of 0.25 to 0.33 μm. At higher calcination temperature (800 °C), the particles seem to fuse together and the sizes ranging from 0.33 to 0.66 μm.

For coprecipitation process (Figure 3.16 [(d)-(f)]), there was a similar trend as in Figure 3.16 [(a)-(c)], at higher calcination temperature, the bigger particle size was occurred. Figure 3.16 (d), at 600 °C, the particles were spherical and the sizes were ranging from 0.17 to 0.25 μm. At 700 °C, the particles became larger and seem to fuse together, their sizes were 0.33 to 0.40 μm. And at 800 °C, there was the particle fusion. Interparticle necks developed and some exaggerated grain growth was occurred. The sizes were between 0.50 to 0.75 μm.

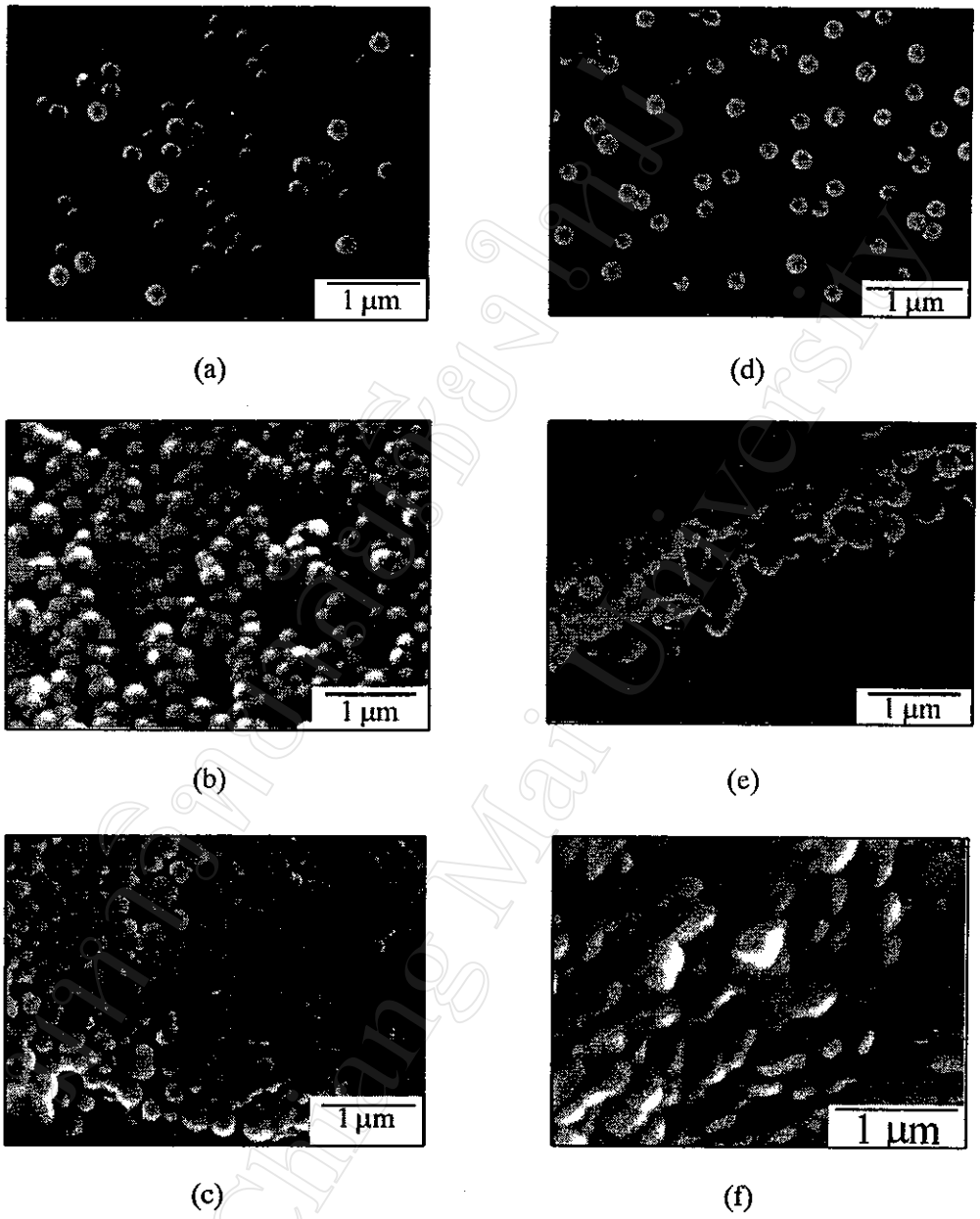

Figure 3.16 SEM micrograps of PZT powders obtained from freeze-drying process calcined for 2 hours at (a) 600 °C, (b) 700 °C, (c) 800 °C, and PZT powders obtained from coprecipitation process calcined for 2 hours at (d) 600 °C, (e) 700 °C and (f) 800 °C.

3.1.3.2 PLZT powders from Nitrate Solutions

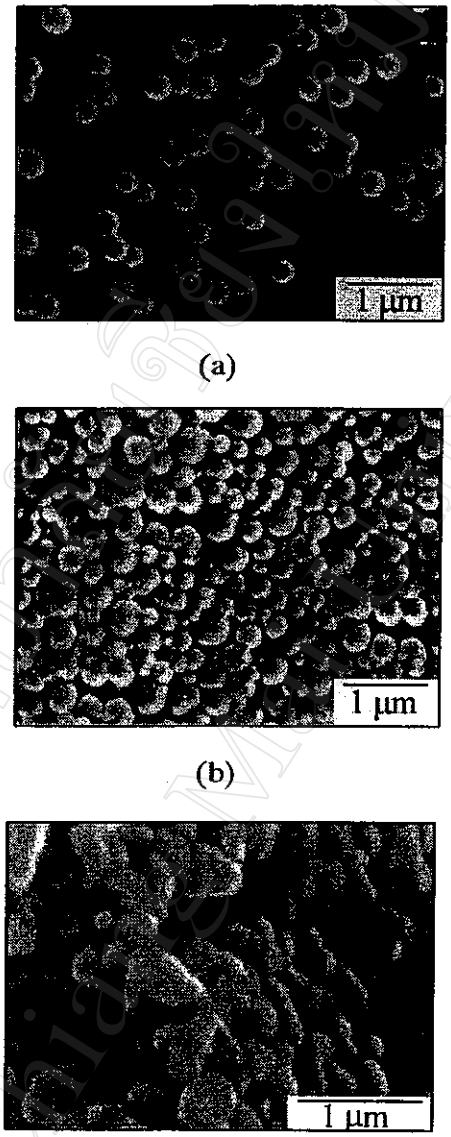

Figure 3.17 SEM micrograps of PLZT powders obtained from coprecipitation process calcined for 2 hours at (a) 600 °C, (b) 700 °C and (c) 800 °C

Figure 3.17 [(a)-(c)] shows SEM micrographs of PLZT powders obtained from coprecipitation process at different calcining temperatures. The calcining temperature and the particle size were increased in the same way. At 600 °C, Figure 3.17(a), the micrograph showed the spherical particles with 0.30 μm to 0.35 μm in diameter. At 700 °C, Figure 3.17 (b), the particles became larger and the sizes ranged from 0.35 μm to 0.50 μm. At 800 °C, Figure 3.17 (c), the particles seem to fuse together, some grain growth occurred and the sizes were between 0.50 μm to about 0.75 μm.

3.1.3.3 PZT Powders from Hydrothermal Process.

3.1.3.3.1 Effect of Mineralizer Concentration

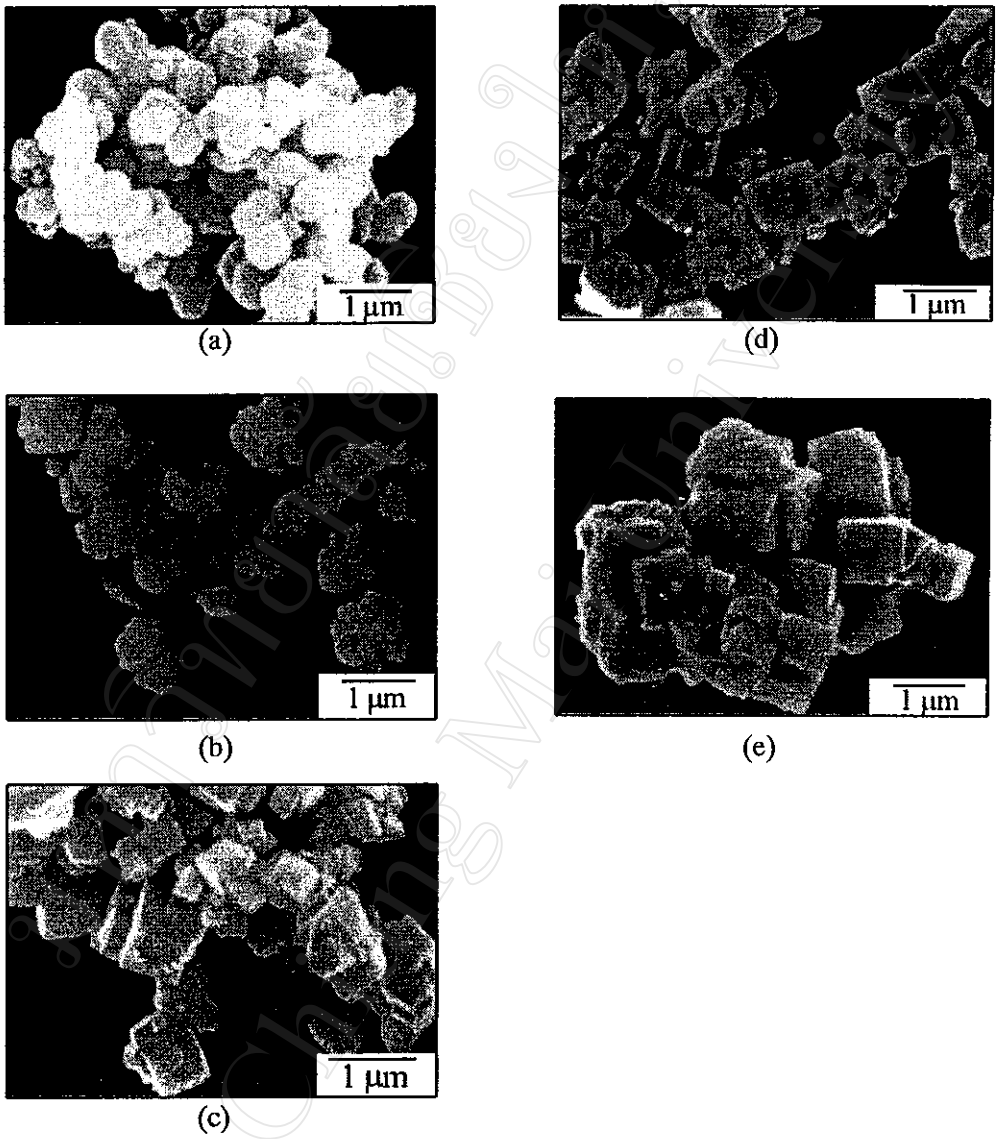

Figure 3.18 SEM micrographs of PZT powders obtained from hydrothermal process at 200 °C for 6 hours using KOH as a mineralizer in different concentrations as (a) 1.0 M, (b) 2.0 M, (c) 3.0 M, (d) 4.0 M and (e) 5.0 M KOH.

Figure 3.18 [(a)-(e)] shows SEM micrographs of PZT powders synthesized by hydrothermal process at 200 °C for 6 hours using KOH as a mineralizer in different molar concentrations. As the KOH concentration increased, the particle size and the agglomeration increased significantly. At 1.0 and 2.0 M KOH, the powders showed pseudocubic forms. At higher molar concentrations (4.0 and 5.0 M KOH), the powders morphology transformed to the cubic particles. The particle size increased from 0.3 - 0.7 μm, (Figure 3.18 (d)), to about 0.75 μm, (Figure 3.18 (e)), when the KOH concentration increased from 4.0 to 5.0 M.

3.1.3.3.2 Effect of Mineralizer Type

SEM micrographs of PZT powders synthesized by hydrothermal process at 200 °C for 6 hours using KOH and NaOH as the mineralizer in different molar concentrations are given in Figure 3.19 [(a)-(f)]. A similar trend occurred with the PZT powders which was using NaOH as a mineralizer. It can be seen from Figure 3.19 (d) to (f) that increasing NaOH concentration from 3.0 to 5.0 M resulted a larger particle sizes with increasing from 0.3 μm to 1.0 μm and agglomeration was formed between the cubic particles. The KOH mineralizer caused larger particle size but in narrower size distribution than when NaOH was used as a mineralizer.

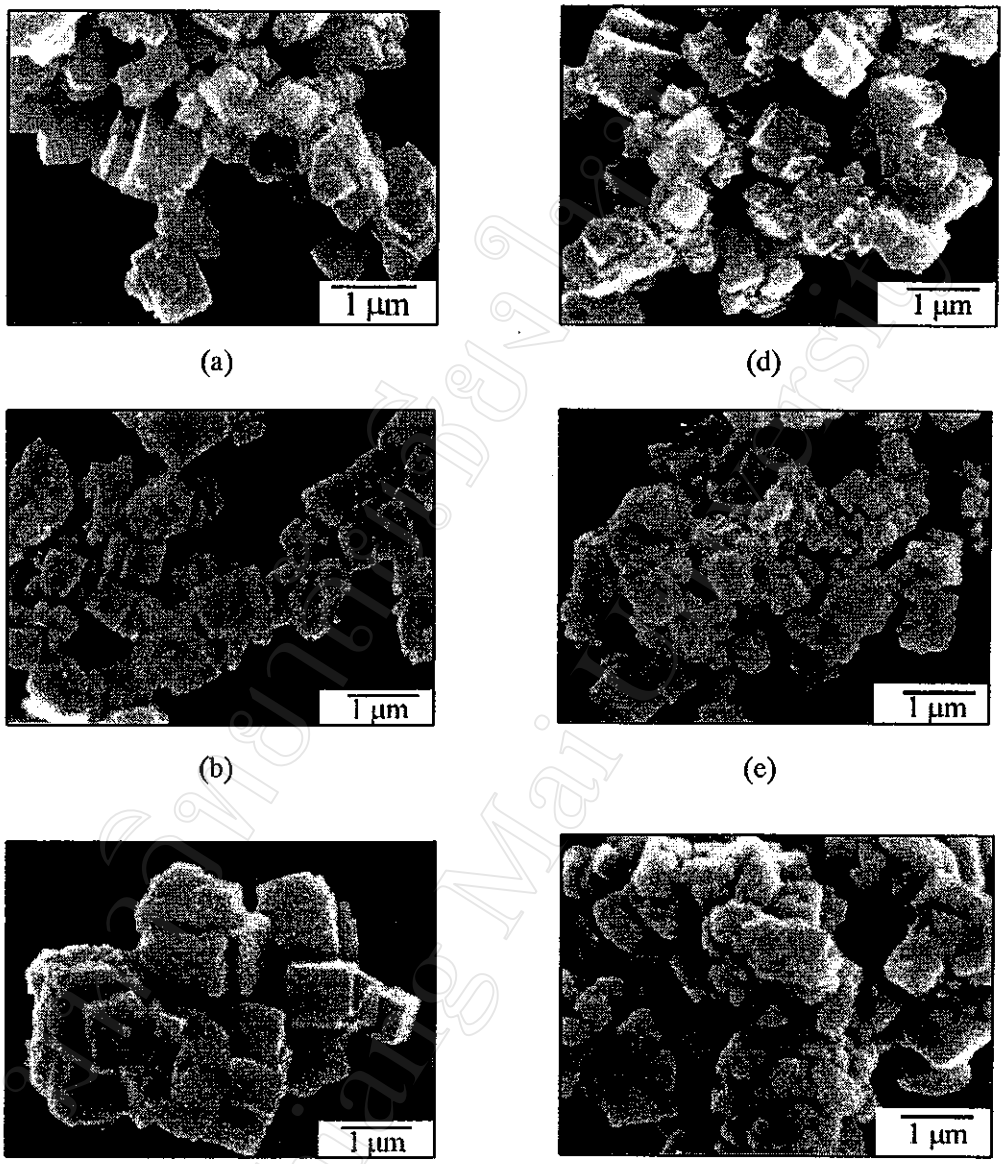

Figure 3.19 SEM micrographs of PZT powders obtained from hydrothermal process at 200 °C for 6 hours in different KOH concentrations as (a) 3.0 M, (b) 4.0 M, (c) 5.0 M and in different NaOH concentrations as (d) 3.0 M, (e) 4.0 M, (f) 5.0 M.

3.1.3.3.3 Effect of pH Value

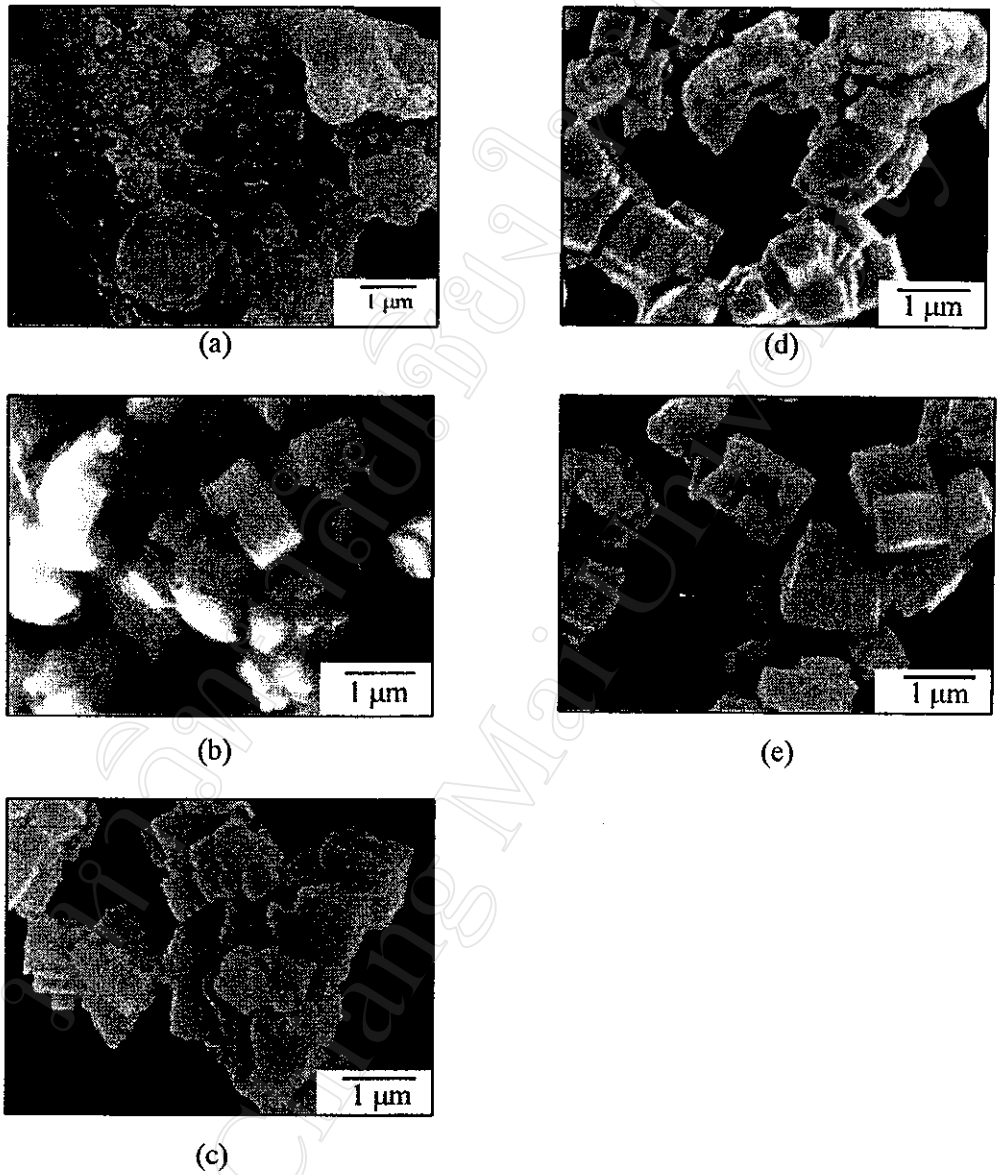

Figure 3.20 SEM micrographs of PZT powders obtained from hydrothermal process at 200 °C for 6 hours using 4.0 M KOH as a mineralizer in different pH values as (a) pH 10, (b) pH 11, (c) pH 12, (d) pH 13 and (e) pH 14

Figure 3.20 [(a)-(e)] shows SEM micrographs of PZT powders synthesized by hydrothermal process at 200 °C for 6 hours using 4.0 M KOH as a mineralizer at different pH values. At low pH value, pH 10 (Figure 3.20(a)), the powders were amorphous and irregular in shape. At pH 11 and 12 [Figure 3.20 (b) and (c)], the products were not completely crystallite and the powder's morphology became the cubic particles. At higher pH value, pH 13 and 14, it can be seen clearly from Figure 3.19 (d) and (e) that the powders were the cubic particles and their sizes ranged between 0.5 μm to 1.0 μm

3.1.3.3.4 Effect of Synthesis Time

SEM micrographs of PZT powders synthesized by hydrothermal process at 200 °C using 4.0 M KOH at pH 14 as a mineralizer at different synthesis time from 2 to 48 hours are illustrated in Figure 3.21 [(a)-(f)]. As the synthesis time increased, both the particle size and the extent of particle agglomeration increased. After synthesis time of 2 and 4 hours, Figure 3.21 (a) and (b), the morphology became more cubic with an increased size of 0.25 μm to 0.33 μm. At the synthesis time of 6 hours and longer, Figure 3.21 (c) to (f), the cubic morphology was fully developed, the particle sizes increased to between 0.33 μm and 1.0 μm but the size distribution of the longer synthesis time was narrower than the shorter synthesis time.

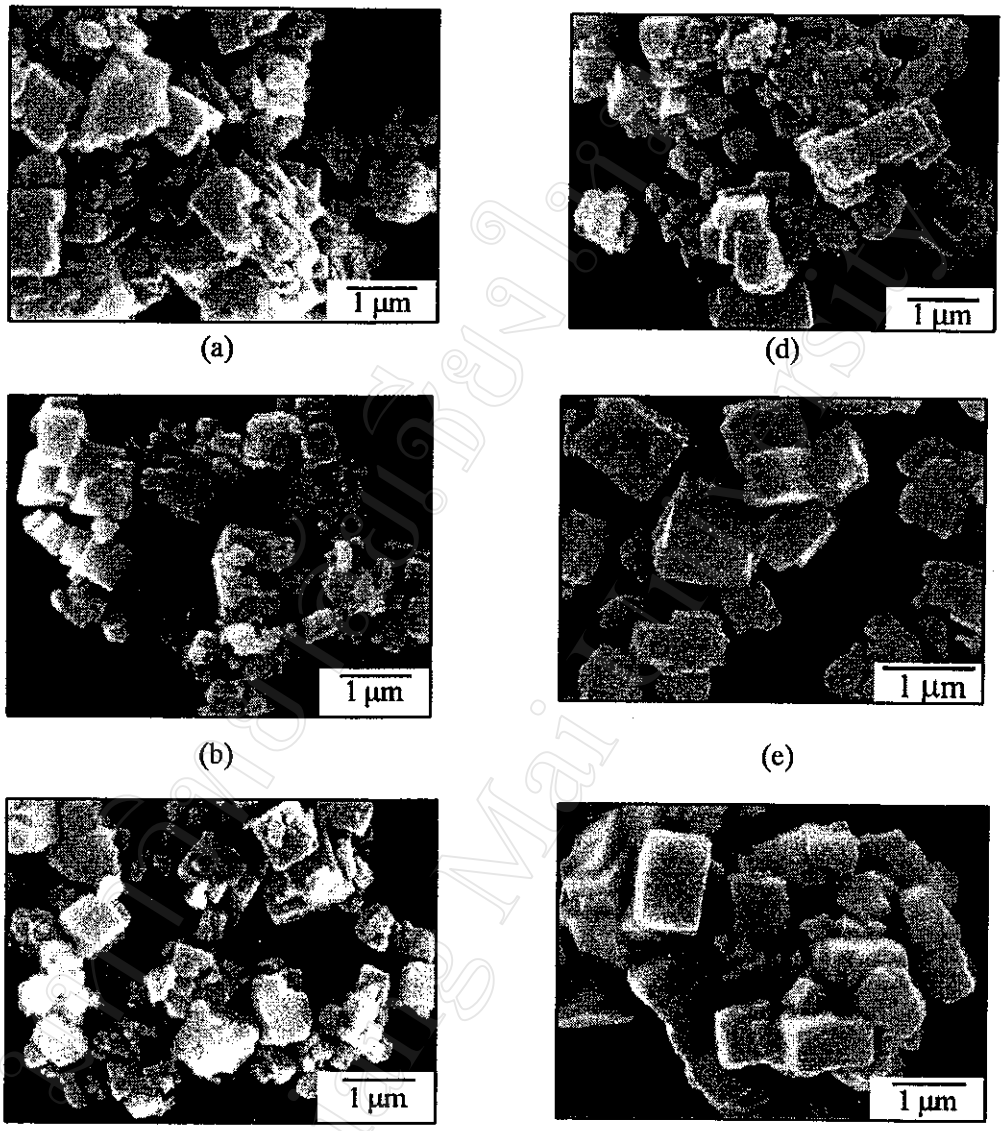

Figure 3.21 SEM micrographs of PZT powders obtained from hydrothermal process at 200 °C using 4.0 M KOH as a mineralizer at different synthesis times as (a) 2 h, (b) 4 h, (c) 6 h, (d) 12 h, (e) 24 h and (f) 48 h.

3.1.3.3.5 Effect of Synthesis Temperature and Time

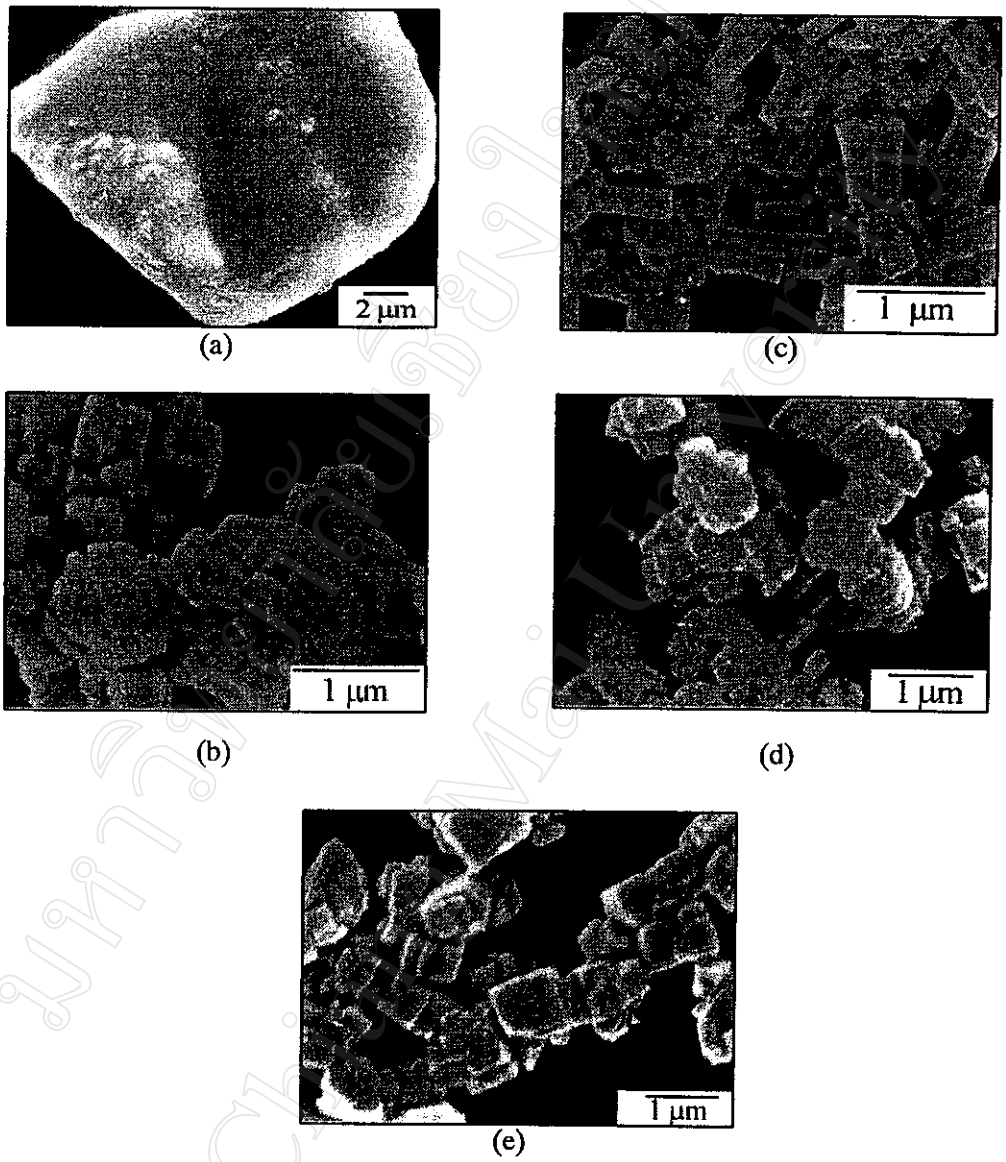

Figure 3.22 SEM micrograps of PZT powders synthesized by hydrothermal process using 4.0 M KOH as a mineralizer at different temperatures and times as (a) 50 °C, 48 h, (b) 100 °C, 48 h, (c) 150 °C, 6 h, (d) 150 °C, 24 h and (e) 200 °C, 6 h

Figure 3.22 shows SEM micrographs of PZT powders obtained from hydrothermal process using 4.0 M KOH as a mineralizer at different synthesis temperatures and times. At relatively low synthesis temperature (at 50 °C) while a long synthesis time was used (48 hours), Figure 3.22 (a), the product was amorphous and irregular in shape. At low synthesis temperature (100 °C) and long synthesis time (48 hours), Figure 3.22 (b), some tabular particles was occurred and there was some agglomerated between these cubic particles, because of the long synthesis time. At relatively high temperature (150 °C) and synthesis time of 6 and 24 hours, (Figure 3.22 (c)), the tabular particles were formed with sizes in the range of 0.5 μm to 0.75 μm and at 150 °C for 24 hours, the cubic particles were formed and there was some agglomeration between these cubic particles. Figure 3.22 (e) shows the PZT particles synthesized at 200 °C for 6 hours. The product showed well crystallite cubic particle with the size of 0.3 μm to 0.7 μm. From this study, it can be seen clearly that the synthesis temperature did not cause the particle agglomeration like the synthesis time had done.

3.1.3.4 PLZT Powders from Hydrothermal Process

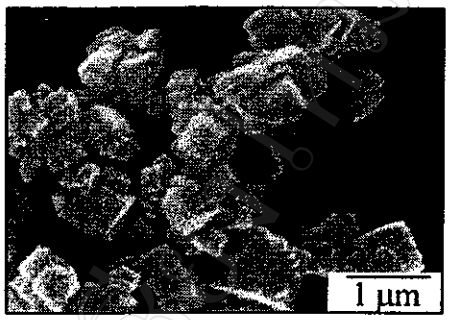

Figure 3.23 SEM micrograph of PLZT powders at 10 %La synthesized by hydrothermal process at 200 °C for 6 hours using 4.0 M KOH as a mineralizer

Figure 3.23 shows SEM micrograph of PLZT powders contained 10 mole % La obtained through hydrothermal process at 200 °C for 6 hours using 4.0 M KOH as a mineralizer. From this micrograph, PLZT powders showed well crystallite product which had cubic shape, and some agglomeration was occurred between the cubic particles. There was the large size distribution, their sizes ranged from 0.33 μm to 1.0 μm.

3.1.3.5 TEM Observation

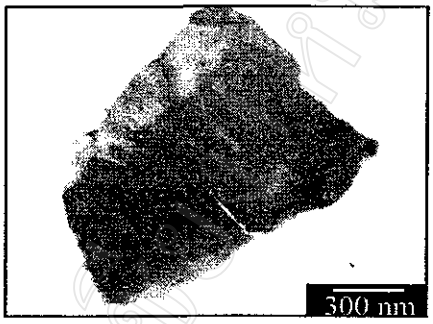

Figure 3.24 TEM micrograph of PZT powders synthesized by hydrothermal process at 200 °C for 24 hours using KOH as a mineralizer

Figure 3.24 shows the TEM micrograph of PZT powders synthesized by hydrothermal process at 200 °C for 24 hours using KOH at pH 14 as a mineralizer. The pattern showed that the powders were well crystallite and the cubic perovskite PZT powders were formed with sizes of 0.5 to 0.75 μm. There was no intermediate phase occurred at this condition. For PZT powders synthesized at low synthesis temperature or low synthesis time, some minor intermediate phase such as acicular or tabular particles were formed. These particles were investigated during hydrothermally synthesis of $PbTiO_3$ [70] and PLZT[91]. The acicular and tabular particles had various Pb and Ti as a major compositions and Zr as a minor composition. The Pb:Ti ratio was 1 for tabular particles, which were $PbTiO_3$ or PZT(T), and less than 1 for acicular particle, which was PbO.

3.1.4 PARTICLE SIZE DISTRIBUTION ANALYSIS

3.1.4.1 PZT Powders from Nitrate Solutions

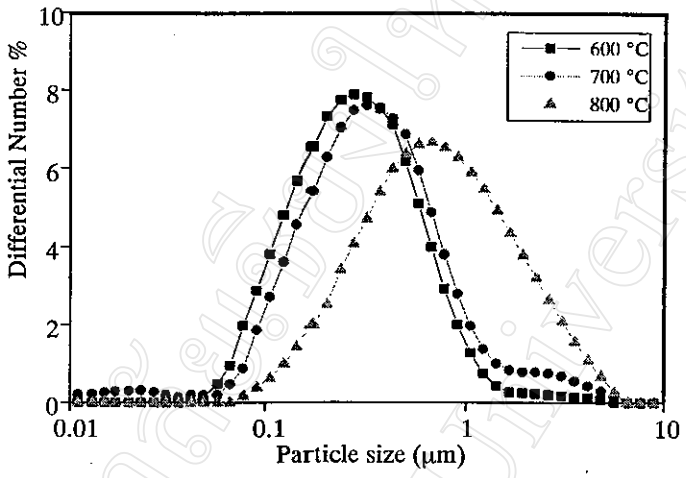

Figure 3.25 Particle size distribution analysis of PZT powders obtained from nitrate solutions calcined at 600 °C, 700 °C and 800 °C

Figure 3.25 shows the particle size distribution of PZT powders obtained through nitrate solutions and calcined at 600 °C, 700 °C and 800 °C for 2 hours. The distrbution curves demonstrated the particle sizes of 0.4, 0.5 and 0.8 μm at calcination temperature of 600, 700 and 800 °C respectively, which were slightly higher than the SEM results (Figure 3.16). The distribution curves of 600 °C and 700 °C calcined powders showed the smaller size and narrower size distribution than that of 800 °C, while the 600 °C calcined powders had a slightly smaller size than that of 700 °C. This study confirmed the same results as SEM analysis (Figure3.16) that the particle size and the extent of particle agglomeration increased with increasing calcination

temperature. The increasing of size distribution of the calcined powders at 800 °C might be occurred because of the particle fusion at high calcination temperature.

3.1.4.2 PZT Powders from Hydrothermal Process

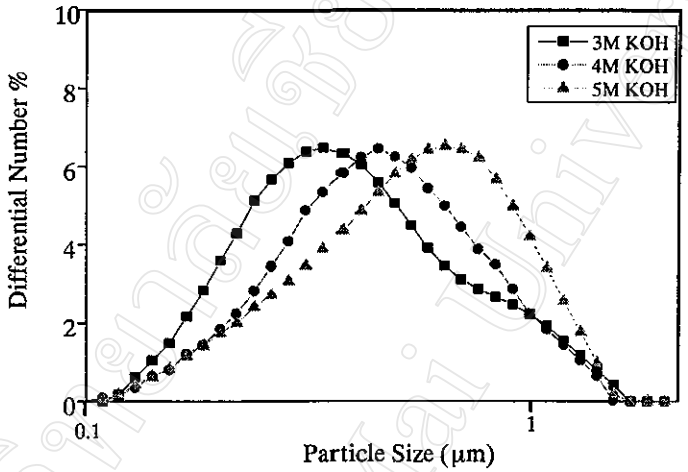

Figure 3.26 Particle size distribution analysis of PZT powders obtained by hydrothermal process at 200 °C for 6 hours using KOH at 3.0 M, 4.0 M and 5.0 M as mineralizer

Particle size distribution curves of PZT powders synthesized by hydrothermal process at 200 °C for 6 hours using KOH as a mineralizer at different molar concentration are shown in Figure 3.26. The distribution curves represented the particle sizes of 0.5, 0.6 and 0.9 μm at the KOH concentrations of 3.0 M, 4.0 M and 5.0 M respectively, which were closed to the SEM results (Figure 3.18). The curves demonstrated that when KOH molar concentrations increased (from 3.0 to 5.0 M), the particle sizes shifted to the larger modal size. And at 4.0 M KOH the curve showed

more symmetry than that of 3.0 and 5.0 M KOH, it should be from the more cubic particles in the particle morphology at this KOH concentration.

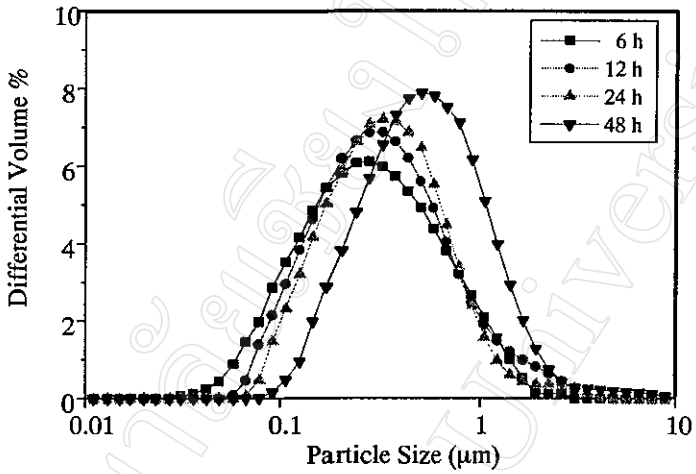

Figure 3.27 Particle size distribution analysis of PZT powders obtained through hydrothermal process at 200 °C using 4.0 M KOH as a mineralizer at different synthesis times of 6 h, 12 h, 24 h and 48 h

Particle size distribution curves of PZT powders synthesized by hydrothermal process at 200 °C using 4.0 M KOH as a mineralizer at different synthesis times are given in Figure 3.27. The distribution curves represented the particle sizes of 0.4, 0.45, 0.5 and 0.7 μm at the synthesis times of 6, 12, 24, and 48 hours respectively, which were closed to the SEM results (Figure 3.21). The distribution curves indicated that when the synthesis time increased the curve became slightly narrower with the increasing of the particle size. The longer synthesis time enabled the particle growth with a narrower size distribution than that of the shorter synthesis time.

3.1.5 FORMATION MECHANISM FOR PZT POWDERS SYNTHESIZED FROM NITRATE SOLUTIONS

Lead zirconate titanate powders have been synthesized by nitrate route. Titanium isopropoxide [$Ti(OC_3H_7)_4$] and zirconium n-propoxide, $Zr[O(CH_2)_2CH_3]_4$, were used as the starting precursors. Ammonia solution was used to hydrolyze these two precursors to the solid form as shown in the following reactions:

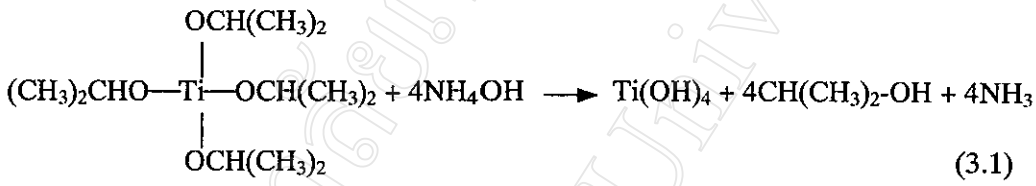

$$(CH_3)_2CHO{-}Ti(OCH(CH_3)_2)_3 + 4NH_4OH \longrightarrow Ti(OH)_4 + 4CH(CH_3)_2\text{-}OH + 4NH_3 \quad (3.1)$$

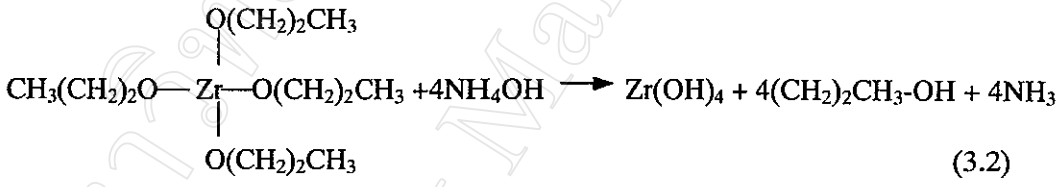

$$CH_3(CH_2)_2O{-}Zr(O(CH_2)_2CH_3)_3 + 4NH_4OH \longrightarrow Zr(OH)_4 + 4(CH_2)_2CH_3\text{-}OH + 4NH_3 \quad (3.2)$$

Titanic acid, [$Ti(OH)_4$] and zirconic acid, [$Zr(OH)_4$] were dissolved in nitric acid to form the titanyl nitrate and zirconyl nitrate, the reactions are as follows:

$$Ti(OH)_4 + 2HNO_3 \longrightarrow TiO(NO_3)_2 + 3H_2O \quad (3.3)$$

$$Zr(OH)_4 + 2HNO_3 \longrightarrow ZrO(NO_3)_2 + 3H_2O \quad (3.4)$$

Hydrogen peroxide solution (30%) was added into the titanyl nitrate and zirconyl nitrate solutions to form the zirconium and titanium nitrate solutions as shown in the following reactions:

$$TiO(NO_3)_2 + H_2O_2 + 2HNO_3 \longrightarrow Ti(NO_3)_4 + H_2O + O_2 + 2H^+ \quad (3.5)$$

$$ZrO(NO_3)_2 + H_2O_2 + 2HNO_3 \longrightarrow Zr(NO_3)_4 + H_2O + O_2 + 2H^+ \quad (3.6)$$

Ammonium hydroxide was used to adjust pH value of the mixed solution between zirconyl nitrate, titanyl nitrate and lead nitrate to be neutral. This clear solution was separated into two parts, the first one was for precipitating method and the second was for freeze-drying method. At pH ~ 7, the amount of ammonium ions was nearly equal to the amount of nitrate ions[92-94].

$$Zr(NO_3)_4 + Ti(NO_3)_4 + Pb(NO_3)_2 \xrightarrow{10\ NH_4OH} Pb(Zr,Ti)O_3 + 10NH_4NO_3 + 10\ OH^- \quad (3.7)$$

$$NH_4NO_3 \longrightarrow N_2O + H_2O \quad (3.8)$$

After freeze-drying or coprecipitation process the $Pb(Zr,Ti)O_3$ products were transformed to PZT powders of the desired composition with the Zr:Ti ratio of 0.52:0.48. For freeze drying process, the solvent was removed to leave a solid residue in which the distribution of cations was substantially the same as in the initial solution[95]. After calcination state the solid residue was decomposed to produce a PZT product.

For coprecipitation process, ammonium hydroxide was further dropped into the cool solution (to prevent some heat which occurred from the reaction)[96]. The pH value of the solution increased rapidly and started to precipitate at pH 10. The solid portion was filtered, washed, calcined and decomposed to PZT powders. From the

thermal decomposition (Figure 3.1), the solid part composed of the $Pb(Zr,Ti)O_3$, some organic residues from the titanium and zirconium precursors, and some of NH_3, NO or NO_2. The organic residues and gases were decomposed and eliminated almost completely at temperature about 600 °C.

The important parameter in nitrate solutions route to produce PZT powders was hydrogen peroxide, H_2O_2. It was used to stabilize titanyl nitrate, $TiO(NO_3)_2$ and zirconyl nitrate, $ZrO(NO_3)_2$ to form titanium nitrate $Ti(NO_3)_4$ and zirconium nitrate $Zr(NO_3)_4$ which were more stable than the titanyl and zirconyl forms. The suitable route for obtaining powders was another important factor. It can be seen from XRD patterns of PZT powders (Figure 3.5 and 3.6), that freeze drying process could produce fine powders with a uniform morphology at a slightly lower calcination temperature (at 600 °C) than the calcination temperature of the coprecipitation process (650 °C). The calcination temperature was also an important factor. High calcination temperature might cause particles growth and particles fusion. Interparticle necks occurred at high calcination temperature, at 800 °C. And above 900 °C, there was the evaporation of lead oxide, which could cause the deficiency of lead, due to the precipitation of ZrO_2 in PZT structure.

3.1.6 FORMATION MECHANISM FOR PZT POWDERS SYNTHESIZED FROM HYDROTHERMAL PROCESS

The Pb, Ti and Zr atoms had different reactions during hydrothermal process. In hydrothermal treatment, lead acetate [$Pb(CH_3COO)_2$. $3H_2O$] reacted with KOH solution, as in the following reaction:

$$Pb(OAc)_2.3H_2O(aq) + 2KOH \longrightarrow PbO(s) + 2KOAc(aq) + 4H_2O(l) \quad (3.9)$$

PbO could be in different forms depending on the pH value of the reaction equilibria[97].

$$PbO(s) + H_2O(l) \longleftrightarrow Pb^{2+}(aq) + 2OH^-(aq) \quad (3.10)$$

$$Pb^{2+}(aq) + H_2O(l) \longleftrightarrow PbOH^+(aq) + H^+(aq) \quad (3.11)$$

$$PbOH^+(aq) + OH^-(aq) \longleftrightarrow Pb(OH)_2(aq) \quad (3.12)$$

$$Pb(OH)_2(aq) + OH^-(aq) \longleftrightarrow HPbO^{2-}(aq) + H_2O(l) \quad (3.13)$$

$$Pb(OH)_2(aq) \longleftrightarrow Pb(OH)_2(s) \quad (3.14)$$

At low pH, reactions (3.10) and (3.11) occur, yielding Pb^{2+} and $PbOH^+$ while $PbOH^+$ was the dominant species[98]. At high pH, reactions (3.12), (3.13) and (3.14) were promoted, the $Pb(OH)_2$ (aq) were precipitated in form of $Pb(OH)_2$ (s). The proposed ABO_3 perovskite formation reaction could be shown as follows[99]:

$$A^{2+}(aq) + B(OH)_6^{2-} \longrightarrow ABO_3(s) + 3H_2O(l) \qquad (3.15)$$

Where A^{2+} is the alkaline earth

B^{4+} is the transition metal cations

Titanium isopropoxide and zirconium n-propoxide could be reacted rapidly with the moisture in the air, the procedure for preparing these two starting precursors in isopropanol should be prepared rapidly or in the closed system such as in the glove box.

It has been reported that the zirconia and titania precursors tended to form polymeric gel, as $[Ti\text{-}O\text{-}Ti]_n$ and $[Zr\text{-}O\text{-}Zr]_n$ than the isolated Ti^{4+} or Zr^{4+} ions except in the strong acidic condition. The Ti^{4+} or Zr^{4+} ions could not actually exist because of its high charge to ionic radius ratio[100]. In this work, the reaction between titanium isopropoxide $[Ti(OC_3H_7)_4]$ and isopropanol (C_3H_8O) led to the following reaction;

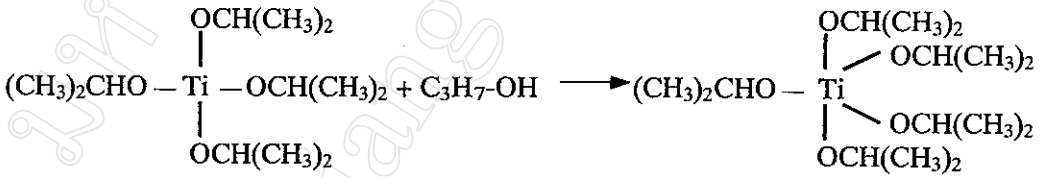

(3.16)

In the excess of isopropanol the following molecular structure might be formed as[101]:

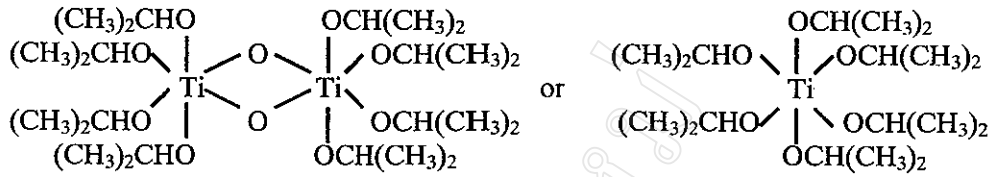

(3.17)

The similar structure had occurred with zirconium n-propoxide $[Zr[O(CH_2)_2CH_3]_4]$ and isopropanol (C_3H_8O) as follows:

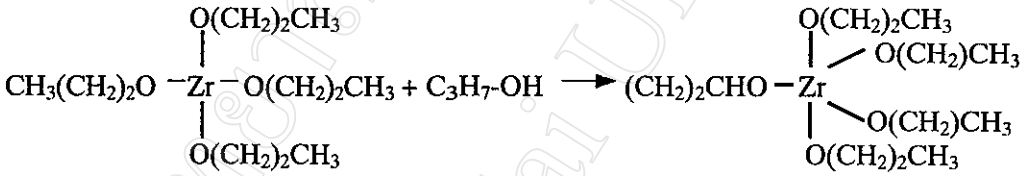

(3.18)

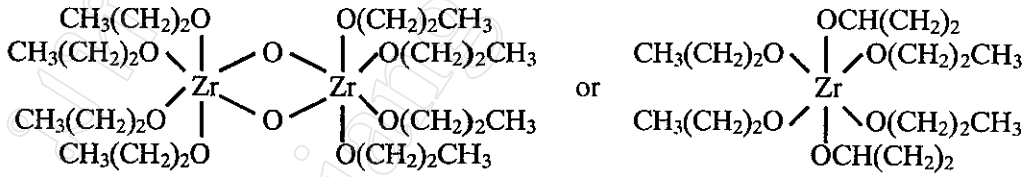

(3.19)

The Ti^{4+} and Zr^{4+} might react with the acetate group in lead acetate, as in the following reactions[102]:

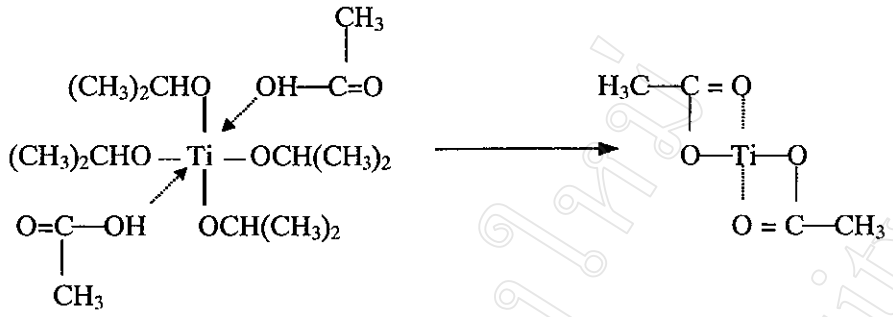

(3.20)

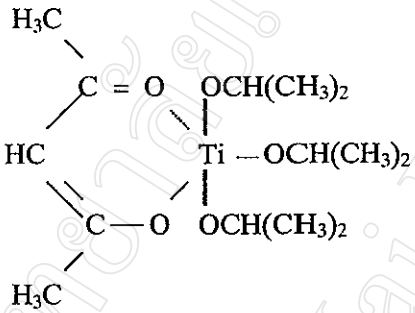

(3.21)

or

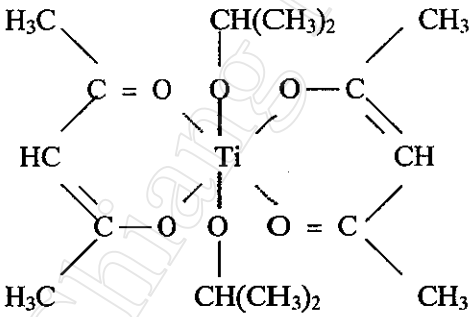

(3.22)

Note that Zr^{4+} ions could occur in a similar reaction and had the same structure as Ti^{4+} ions.

During these reactions the coordination number of titanium and zirconium ions increased from four to six with the low molecular weight oligomeric species being formed in the hydrothermal process. In the hydrothermal treatment, some

condensation might be occurred, which was the formation of fibrous titania and zirconia gels[103] or some polyhedral crystal structure depending on the synthesis conditions. And the solubility of the titania and zirconia gel would decrease with the increasing of the synthesis temperature[104].

The temperature of forming PZT was lower than that of $PbTiO_3$ or $PbZrO_3$ under the same condition, such as at synthesis time of 6 hours, reaction medium of 4.0 M KOH, PZT could be formed at 150 °C while $PbTiO_3$ or $PbZrO_3$ could be formed at about 170 °C and 220 °C respectively. The above results indicated that PZT was formed directly, instead of substitution of Zr^{4+} for Ti^{4+} in $PbTiO_3$ [78].

The significant feature of the PZT amorphous gels, when Ti-O-Ti and Zr-O-Zr linkages were formed, is the Ti-O-Zr bonding only formed in a small fraction in the network system[105]. The Pb cations did not participate in the bonding with Ti and Zr atoms but they occupied random positions within the titania-zirconia gels. The mineralizer played an important role during the hydrothermal treatment. The smaller the mineralizer cation radius, the more easily it would diffuse into the gel network, causing the bond rupture, and the more effective it would be in assisting the nucleation of PZT[106]. During hydrothermal treatment, K^+ ions (in KOH) caused chemical changes and the rupture of Ti-O-Ti or Zr-O-Zr bridging bonds as shown below;

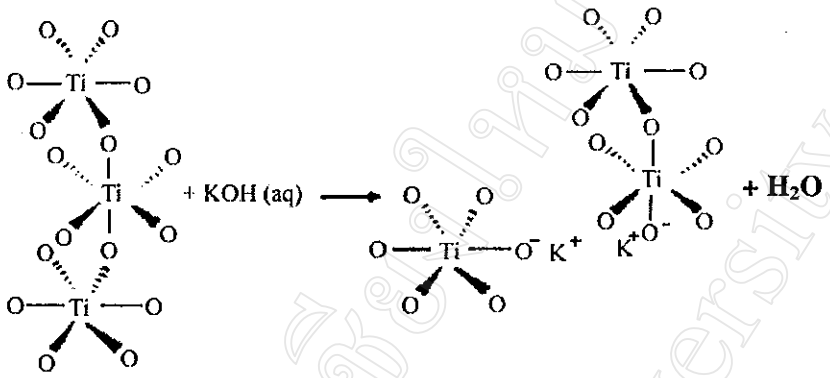

(3.23)

And the organic groups (propoxide group, OPr) continued to be replaced by hydroxyl groups, leading finally to the heterogeneous nucleation within the gel. The possible formation process is shown in Figure 3.28[106].

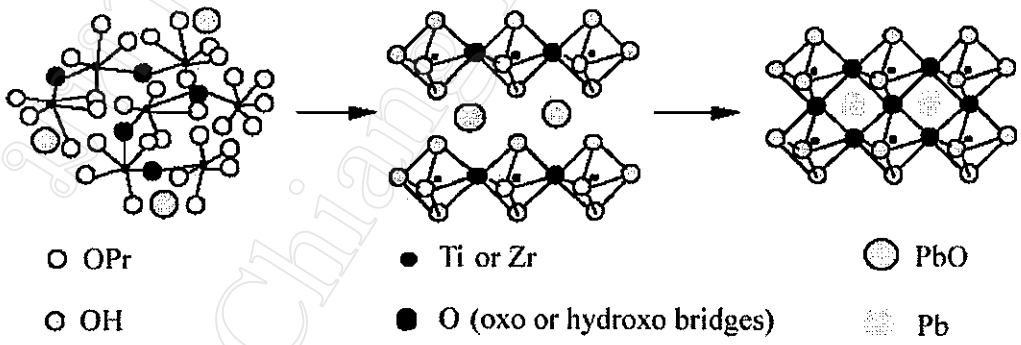

Figure 3.28 Schematic representation of the perovskite PZT particle formation process[106].

The important parameters in hydrothermally synthesized PZT powders were mineralizer type and concentration, synthesis temperature and synthesis time. The mineralizer concentration used in the reaction should be in the minimum necessary concentration to ensure phase pure perovskite particles formation. Increasing mineralizer concentration would lead to polynuclear growth, which was the agglomerated of the cubic PZT particles. An increase in the solubility of Zr^{4+}, Ti^{4+} and Pb^{2+} while increasing concentration of mineralizer (at 5.0 M KOH), could accelerate the process of recrystallization. This process would homogenize the composition of PZT product and might lead to the larger particle size. Increasing synthesis temperature could reduce the minimum mineralizer concentration required for PZT formation, thus reducing the agglomerate particle size. Increasing synthesis time could lead to a narrower size distribution but agglomeration between some cubic particles could occur. For hydrothermal vessel which had a teflon line cup inside, the synthesis temperature could not be more than 250 °C which was the melting point of the teflon plastic. Above this temperature, the teflon line cup was melt and produced F_2 and CO gasses which were danger for human being.

3.1.7 IMPURITIES DETERMINATION

Trace impurities in nitrated PZT powders were analyzed by atomic absorption spectrophotometry. Impurity contents in PZT powders calcined at different temperatures are shown in Table 3.1. The average mass percent of sodium (Na) and magnesium (Mg) ranged from 0.022 to 0.037. No potassium (K), calcium (Ca) or strontium (Sr) ions were found in PZT powders. The average impurities in PZT powders was 0.035±0.007 ppm.

Table 3.1 Trace impurites in the PZT powders

Calcination Temperature (°C)	Impurity content (ppm)					Total (ppm)
	Na	K	Mg	Ca	Sr	
550	0.034	ND	0.002	ND	ND	0.036
600	0.033	ND	0.002	ND	ND	0.035
650	0.024	ND	0.001	ND	ND	0.025
700	0.020	ND	0.002	ND	ND	0.022
750	0.030	ND	0.001	ND	ND	0.031
800	0.032	ND	0.002	ND	ND	0.034
Detection Limit	0.002	0.005	0.001	0.003	0.017	-

*ND is non detectable

3.1.8 LEAD TO ZIRCONIUM TO TITANIUM RATIO IN PZT POWDERS

The amounts of lead (Pb), zirconium (Zr) and titanium (Ti) at different calcination temperature in nitrated PZT powders were determined as described in Chapter 2 (2.4.7). Table 3.2 shows the mole ratio of lead to zirconium to titanium in PZT powders in each calcination temperature. The average mole ratio of Pb:Zr:Ti in PZT powders was 1:0.525:0.487 ± 0.006:0.001, which was close to the desired composition of the final materials.

Table 3.2 Lead to zirconium to titanium ratio in PZT powders

Calcination Temperature (°C)	Results (mol×10^3)			Mole Ratio of Pb:Zr:Ti
	Pb	Zr	Ti	
Calculated	15.355	7.985	7.370	1:0.52:0.48
550	14.401	7.632	7.056	1:0.53:0.49
600	15.582	8.258	7.453	1:0.52:0.48
650	14.455	7.656	6.933	1:0.53:0.48
700	14.972	7.935	7.186	1:0.53:0.48
750	15.166	7.866	7.431	1:0.52:0.49
800	15.327	7.973	7.633	1:0.52:0.50

3.2 CERAMICS CHARACTERIZATION

3.2.1 Densification of PZT ceramics

The PZT powders from nitrate solutions calcined at 600 °C for 2 hours and the PZT powders from hydrothermal process at synthesis temperature of 200 °C for 6 hours using 4.0 M KOH as a mineralizer were selected for densification measurements because of their similar rhombohedral structure. PZT powders from both processes were pressed and sintered at the temperature between 1000 °C to 1250 °C for 3 and 5 hours. Their results are illustrated in Table 3.3.

The theoretical density of the rhombohedral PZT, estimated from the lattice parameters, was 8.085 g/cm^3 and the theoretical density of the tetragonal PZT was 8.006 g/cm^3, so the average theoretical density used for calculations %theoretical average density was 8.045 g/cm^3. The sintered pellet density was measured by an immersion technique and calculated from the Archimedes' principle.

From Table 3.3, the suitable sintering temperature for PZT ceramics obtained from coprecipitation process was 1150 °C for 5 hours because at lower sintering temperatures and times the ceramics were less dense, while at higher sintering temperatures and times, there was no density change. For PZT ceramics obtained from hydrothermal process, suitable sintering temperature was 1250°C for 5 hours.

Table 3.3 The measured density, % theoretical density, % porosity and % linear shrinkage of PZT powders obtained from nitrate solutions and hydrothermal process.

Method	Sintering temperature (°C)	Sintering time (h)	Measured density (g/cm^3)	Theoretical density (%)	Porosity (%)	Linear shrinkage (%)
Nitrate solutions	1000	3	5.78	71.84	28.16	7.32
	1100	3	6.84	85.02	14.98	10.04
	1150	3	7.48	92.97	7.03	12.36
	1200	3	7.45	92.60	7.40	12.32
	1250	3	7.40	91.98	8.02	12.30
	1000	5	5.90	73.33	26.67	7.74
	1100	5	6.98	86.76	13.24	10.51
	1150	5	7.58	94.32	5.68	12.44
	1200	5	7.50	93.23	6.77	12.41
	1250	5	7.43	92.35	7.65	12.43
Hydrothermal process	1000	3	5.54	68.85	31.15	9.12
	1100	3	6.02	74.82	25.18	11.07
	1150	3	6.58	81.78	18.22	12.97
	1200	3	7.32	90.99	9.01	13.25
	1250	3	7.44	92.47	7.53	13.48
	1000	5	5.67	70.47	29.53	9.99
	1100	5	6.14	76.31	23.69	11.55
	1150	5	6.69	83.15	16.85	13.01
	1200	5	7.43	92.35	7.65	13.32
	1250	5	7.62	94.71	5.29	13.5

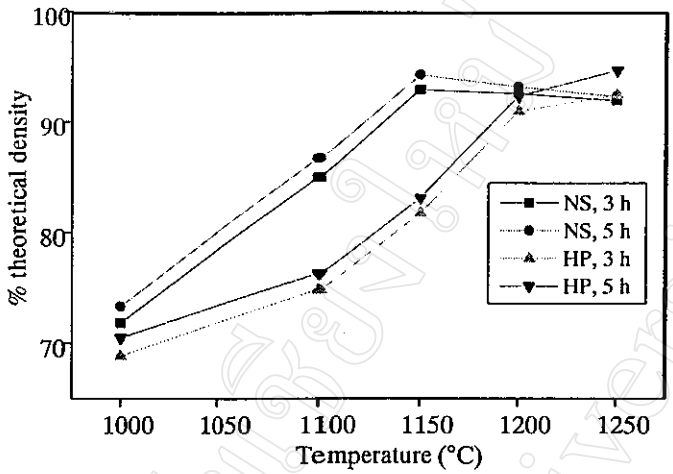

Figure 3.29 Percent theoretical density versus sintering temperature curves at sintering time of 3 and 5 hours for both nitrate solutions (NS) and hydrothermal process (HP).

Percent theoretical density versus sintering temperature curves at sintering time of 3 and 5 hours for both nitrate solutions and hydrothermal process are shown in Figure 3.29. The suitable sintering temperature for nitrate solutions PZT powders was significantly lower than that for hydrothermal PZT. The sintered density of nitrated-PZT increased rapidly until a temperature of 1150 °C and then decreased slightly with the sintering temperature. For nitrated-PZT, the finer particle size and narrower particle size distribution was due to the increasing abruptly of the sintering temperature at the range of 1000 °C to 1150 °C. While for hydrothermally synthesized PZT, the density increased correspondingly and reached the maximum at temperature of 1250 °C which was higher than nitrated-PZT.

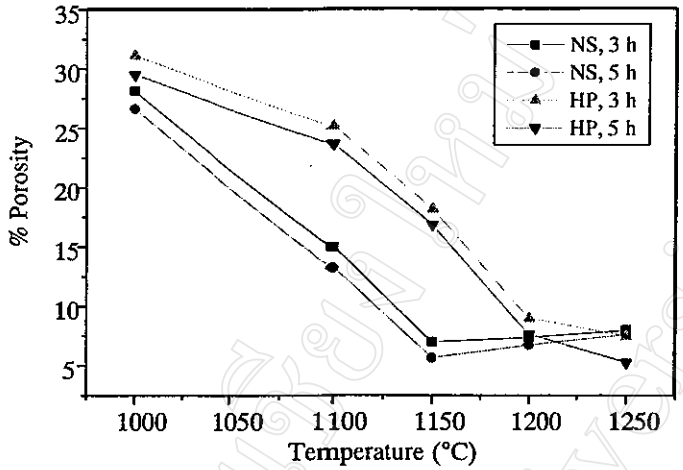

Figure 3.30 Percent porosity versus sintering temperature curves at sintering time of 3 and 5 hours for both nitrate solutions (NS) and hydrothermal process (HP)

Percent porosity versus sintering temperature curves at sintering time of 3 and 5 hours for both nitrate solutions and hydrothermal processes are illustrated in Figure 3.30. Percent porosity was indirect proportionation to % theoretical density. As the sintering temperature increased, % porosity within the pellets decreased while %theoretical density increased. From the curves, % porosity in nitrated-PZT decreased rapidly (% theoretical density increased), at the sintering temperature raising from 1000 to 1150 °C, above 1150 °C, %porosity in nitrated-PZT increased slightly. For hydrothermally synthesized PZT, % porosity within the pellets decreased continuously until the sintering temperature of 1250 °C which was the suitable sintering temperature. At this temperature, density of hydrothermally synthesized PZT ceramic increased to its maximum density at 94.71 % theoretical and at 5.29 % porosity.

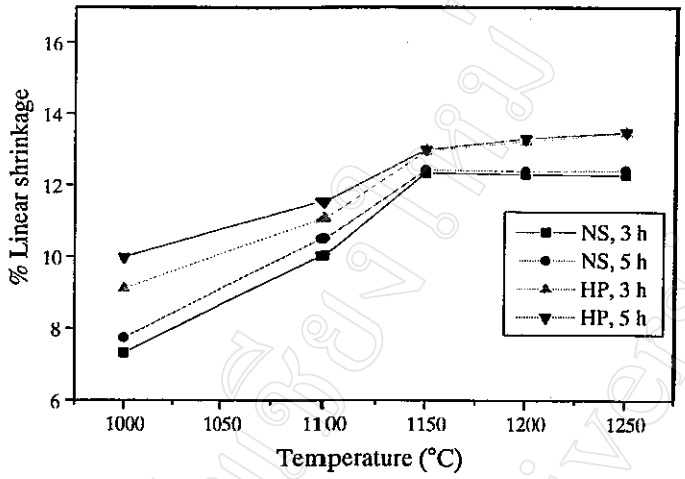

Figure 3.31 Percent linear shrinkage versus sintering temperature at sintering time of 3 and 5 hours for both nitrate solutions (NS) and hydrothermal process (HP).

Percent linear shrinkage versus sintering temperature curves at sintering time of 3 and 5 hours for both nitrate solutions and hydrothermal process are given in Figure 3.31. The curves showed that hydrothermally synthesized PZT had a higher shrinkage percent than that of nitrated-PZT. The shrinkage in PZT ceramics had a closed relationship with the weight losses (see Figure 3.1 and 3.3). And weight loss during sintering mainly occurred from the evaporation of lead oxide. This experiment indicated that the nitrated-PZT had a stable crystallized structure for sintering process than hydrothermally synthesized PZT.

3.2.2 XRD patterns of PZT Ceramics

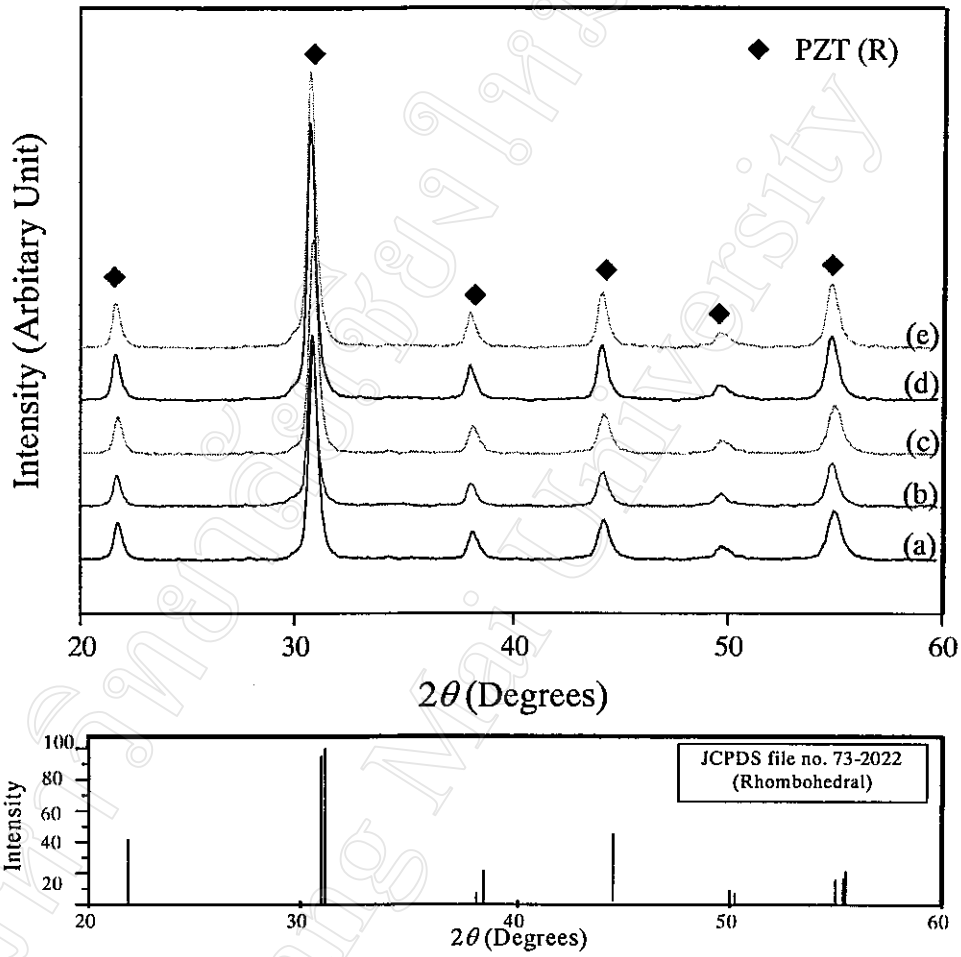

Figure 3.32 XRD patterns of sintered PZT ceramics obtained from coprecipitation process for 5 hours at different sintering temperatures at (a) 1000 °C, (b) 1100 °C, (c) 1150 °C, (d) 1200 °C and (e) 1250 °C

XRD patterns of sintered PZT ceramics obtained from coprecipitation process at different sintering temperatures from 1000 °C to 1250 °C for 5 hours are shown in Figure 3.32. XRD results showed that nitrated-PZT ceramics displayed a

rhombohedral structure whereas the sintering temperature as high as 1250 °C. The shift in crystal structure of PZT ceramics from rhombohedral to tetragonal was occurred from the evaporation of lead oxide due to the precipitation of ZrO_2 in PZT structure[107]. These XRD results confirmed that PZT powders obtained from nitrate solutions had a well-crystallized structure, and this structure was much more stable against lead loss during sintering.

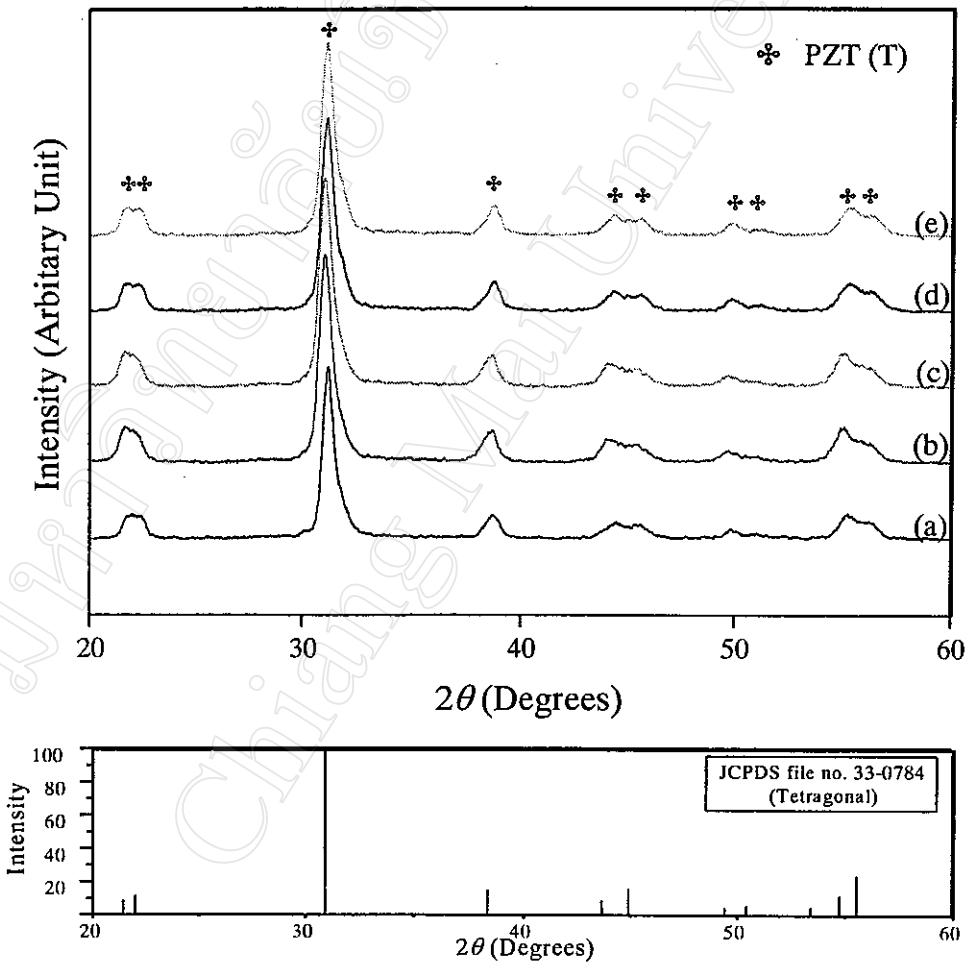

Figure 3.33 XRD patterns of sintered PZT ceramics obtained from hydrothermal process for 5 hours at different sintering temperatures at (a) 1000 °C, (b) 1100 °C, (c) 1150 °C, (d) 1200 °C and (e) 1250 °C

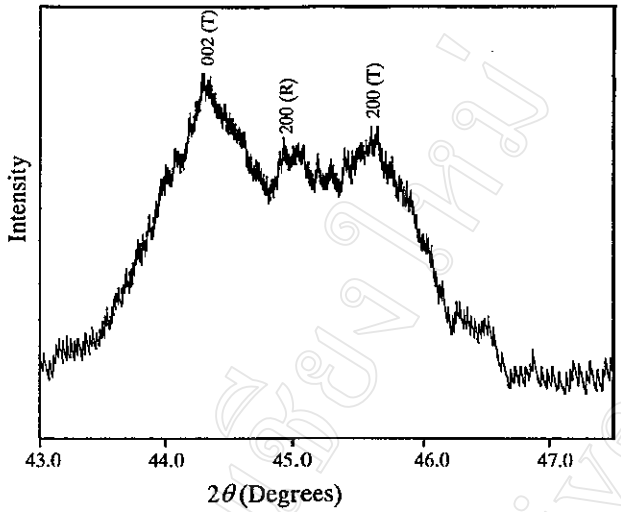

Figure 3.34 Fine structure in XRD pattern of PZT ceramics obtained from hydrothermal process sintered at 1250 °C at 2θ from 43 to 47 degrees

XRD patterns of hydrothermally synthesized PZT at different sintering temperatures are given in Figures 3.33 and 3.34. XRD patterns indicated that, as sintering temperature increased, the peaks at 2θ nearly 45 degree splitted into three peaks of 200 (T), 002 (T) and 200 (R) for the coexisted phases between tetragonal and rhombohedral structures[108, 109]. This split peak did not occur in the initial hydrothermally synthesized PZT powders (Figure 3.10 (d)). The change in the crystal structure of PZT ceramics from rhombohedral to tetragonal was due to the loss of lead oxide which was resulting in the precipitation of ZrO_2. This moved the compositions from MPB towards the ZrO_2 - PZT region[107]. Although the ZrO_2 reflection was not shown in the XRD results, probably because of its content was below the XRD detection limit or its crystal size was too small (<10 nm).

These results could confirm by thermogravimetric analysis of PZT powders (Figure 3.1 and 3.3). The thermal decomposition of nitrated-PZT was almost

completed above 600 °C while hydrothermally synthesized PZT lost its second weight at about 900 °C

3.2.3 Microstructure of PZT ceramics

The microstructure and grain size of the sintered samples were studied using scanning electron microscopic technique. The series of SEM micrographs of PZT from nitrate solutions sintered at 1000 °C to 1150 °C for 5 hours are shown in Figure 3.35. At a sintering temperature of 1000 °C, the microstructure of PZT ceramics from nitrate solutions exhibited a porous structure with no distinct of grain boundary structure, Figure 3.35 (a). At higher sintering temperature, a higher sintered density was observed. For the sintered temperature of 1100 °C, Figure 3.35 (b), the grain size was doubled from 0.75 μm to 1.0 μm at 1000 °C to about 1.5 μm to 2.0 μm at 1100 °C, and the smaller grains were surrounding by the larger ones. At 1150 °C, Figure 3.35 (c), the ceramics showed clear grain boundaries on its surface with its density increased to 94.32 % theoretical. At high grain growth rates, pores became trap within the grains whereas at slow rate of grain growth, the pores could diffuse out to the boundaries and be eliminated[110].

Figure 3.36 shows SEM micrographs of PZT ceramics obtained from hydrothermal process sintered at 1150 °C to 1250 °C for 5 hours. The microstructure of hydrothermal PZT showed the same sintering behavior as PZT ceramics from nitrate solutions but at higher sintering temperature. At 1150 °C, Figure 3.26 (a), the

(a)

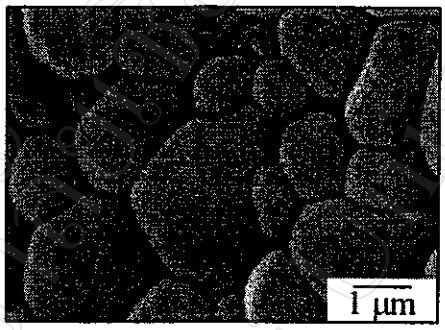

(b)

(c)

Figure 3.35 The series of SEM micrographs of PZT from nitrate solutions sintered for 5 hours at (a) 1000 °C, (b) 1100 °C and (C) 1150 °C

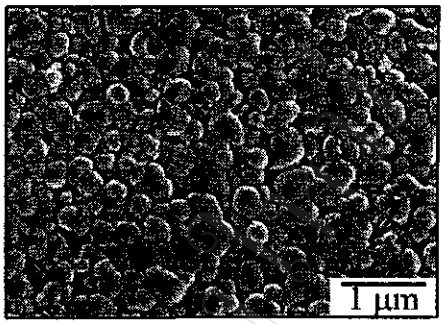

(a)

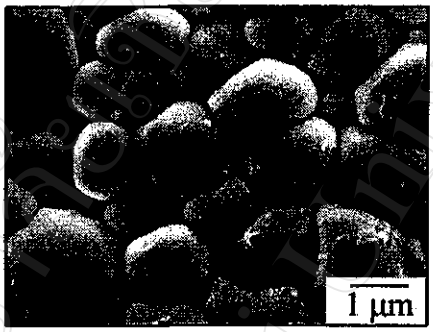

(b)

(c)

Figure 3.36 SEM micrographs of PZT ceramics obtained from hydrothermal process sintered for 5 hours at (a) 1150 °C, (b) 1200 °C and (C) 1250 °C

microstructure exhibited some porous structure. At 1200 °C, Figure 3.26 (b), the microstructure exhibited the bigger grain size with smaller pores than the PZT sintered at 1150 °C. The grain sizes increased to 1.0 μm - 1.5 μm. Finally, when the sintering temperature was raised to 1250 °C, the density increased to 94.71 % and the grain sizes were in the range of 3 μm to 5 μm

The process of sintering contained two classes of mass transportation mechanisms, surface transport and bulk transport[111]. Surface transport involved neck growth without a change in particle spacing (no densification) due to mass flow originated and terminated at the particle surface. Surface diffusion controlled sintering while the bulk transport controlled sintering results in shrinkage. From the above results, nitrated-PZT had the same sintering behavior as hydrothermally synthesized PZT but at a lower sintering temperature. This might be due to the size of the nitrated PZT powders. From Figure 3.16 and 3.25, the nitrated-PZT powders calcined at 600 °C possessed a finer particle size due to the uniform densification at lower sintering temperature. Smaller particles exhibited faster neck growth because of their larger surface energy and needed lower sintering temperature or shorter sintering time.

Hydrothermally synthesized PZT powders synthesized at 200 °C for 6 hours using KOH as a mineralizer was chosen for making the pellets. The PZT powders at this condition exhibited the larger particle sizes (Figure 3.18 (d)) than PZT powders from nitrate solutions that was the reason why hydrothermally synthesized PZT required higher sintering temperature than the nitrated-PZT.

3.2.4 Hot Pressing of PLZT Ceramics

24 g of PLZT powders contained 9% and 10% lanthanum were sent to Fraunhofer Institute for Ceramics Technology and Sinter Work (Fraunhofer Institut fuer Keramische Technologien and Sinterwerkstoffe) in Dresden, Germany. The powders were put in graphite mold. The conditions for hot pressing were 1250 °C for 4 hours at 30 MPa under argon atmosphere. After hot pressing, the product were cut off and polished. SEM was used to study microstructure of PLZT ceramics.

Figure 3.37 shows SEM micrographs of PLZT ceramics contained 9 mole % lanthanum after hot pressing process. In Figure 3.37 (a), the micrograph showed no obvious of transparent PLZT ceramics. It contained the porous structure, contaminated with carbon (from graphite) which was used as a mold. In Figure 3.37 (b), inside the porous structure, the evidence of the improved bond between grains occurred. A predominantly feature surface of this micrograph was the high degree of intergranular fracture surface. This type of fracture occurred in polycrystalline materials only when the grains were strongly and intimately bonded[112]. The pore was entrapped during hot pressing and be as a sink for vacancies and residual porosity in the adjacent porosity[113]. This situation would occur during hot pressing process when the sample was allowed to sinter partially at temperature without external pressure or moderate soaking time. At this hot pressing condition, the pressure was sufficient to cause rearrangement of all the individual particles. The pore free area would be significantly more transparent in PLZT ceramics. This was because the residual particles caused lightscattering which could be a primary source of reduced transparency in the materials[112]. The typical hot pressing conditions for

transparent PLZT were 1250 °C for 16 hours at 14 MPa[17] or under oxygen atmosphere at 1200 °C for 60 hours[114, 115].

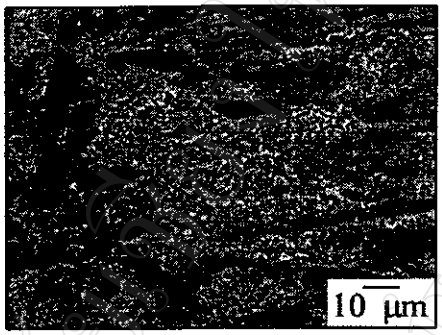

(a)

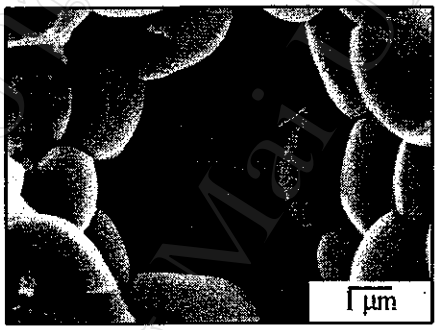

(b)

Figure 3.37 SEM micrographs of PLZT ceramics after hot pressing process (a) the surface structure and (b) the porous structure

3.2.5 Dielectric Properties

The dielectric constants of PZT and PLZT from both nitrate solutions and hydrothermal process were measured at room temperature at the frequencies of 100 Hz to 1 MHz are given in Figure 3.38.

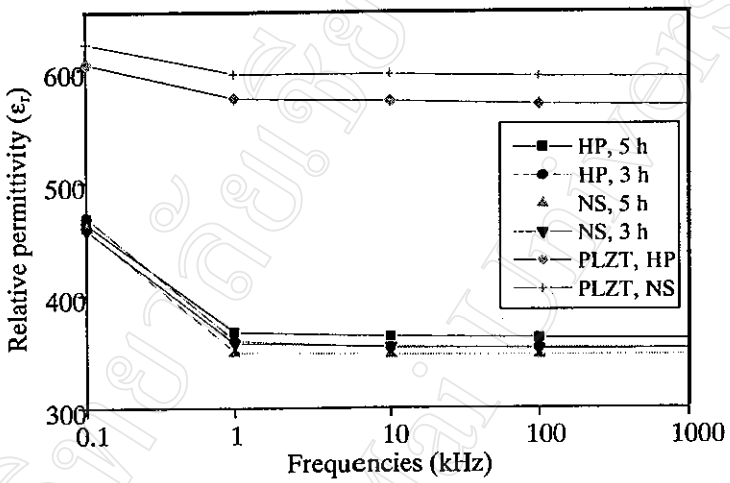

Figure 3.38 Dielectric constant of PZT and PLZT ceramics from nitrate solutions (NS) and hydrothermal process (HP) at different frequencies from 100 Hz to 1 MHz

The dielectric constant or relative permittivity (ε_r) of PZT ceramics from both nitrate solutions and hydrothermal process were found to be about 475 at frequencies of 100 Hz, and about 350 at the frequencies of 1 kHz to 1 MHz. Above 1 kHz, the relative permiitivities were constant. And the dielectric constant of hydrothermally synthesized PZT was slightly higher than that of nitrated-PZT, may be hydrothermally synthesized PZT had a slightly higher density than that of nitrated-PZT.

For PLZT ceramics from both processes, their relative permittivity were constant above 1 kHz at 580 for nitrated-PLZT and at 610 for hydrothermally synthesized PLZT. Comparing dielectric constant values of 10%La doped PZT were higher than that of undoped PZT ceramics. The reason for this behavior was that when PZT ceramics was doped with soft dopant such as lanthanum, the doping ions would occupy in A-sites (replaced in Pb^{2+}). When Pb^{2+} which had smaller ionic radii than La^{3+} were replaced, the extra positive charges (+1) were introduced into the lattice and a Pb vacancy was created in the lattice to maintain electroneutrality [116]. These Pb vacancies caused the transfer of atoms easier than in a perfect lattice, thus the dielectric constant was higher in comparison to the undoped PZT ceramics.